

Formulation and Synthesis of Hexagonal Prism Array Using Nature Inspired Algorithm

Pawan Kumar



Department of Electrical Engineering
National Institute of Technology, Rourkela
Rourkela-769008, Odisha, INDIA

May 2014

Formulation and Synthesis of Hexagonal Prism Array Using Nature Inspired Algorithm

A thesis submitted in partial fulfillment of the
requirements for the degree of

Master of Technology by Research
in
Electrical Engineering

by

Pawan Kumar
(Roll-212EE1209)

Under the Guidance of

Prof.K. R. Subhashini



Department of Electrical Engineering
National Institute of Technology, Rourkela
Rourkela-769008, Odisha, INDIA

2012-2014



Department of Electrical Engineering
National Institute of Technology, Rourkela

C E R T I F I C A T E

This is to certify that the thesis entitled "Formulation and Synthesis of Hexagonal Prism Array Using Nature Inspired Algorithm" by Mr. PAWAN KUMAR, submitted to the National Institute of Technology, Rourkela (Deemed University) for the award of Master of Technology by Research in Electrical Engineering, is a record of bonafide research work carried out by him in the Department of Electrical Engineering, under my supervision. I believe that this thesis fulfils part of the requirements for the award of degree of Master of Technology by Research. The results embodied in the thesis have not been submitted for the award of any other degree elsewhere.

Prof.K. R. Subhashini

Place:Rourkela

Date:

TO MY LOVING PARENTS,MY BROTHERS AND INSPIRING GUIDE

Acknowledgements

First and foremost, I am truly indebted to my supervisors Professor K. R. Subhashini for their inspiration, excellent guidance and unwavering confidence through my study, without which this thesis would not be in its present form. I also thank them for their gracious encouragement throughout the work.

I express my gratitude to the members of Masters Scrutiny Committee, Professors D. Patra, S. Das, P. K. Sahoo, Supratim Gupta for their advise and care. I am also very much obliged to Head of the Department of Electrical Engineering, NIT Rourkela for providing all the possible facilities towards this work. Thanks also to other faculty members in the department.

I would like to thank SURENDRA KUMAR BAIRWA, ARPIT KUMAR BARANWAL, JOSHI KATTA, NIT Rourkela, for their enjoyable and helpful company I had with. I would like to thank also to my seniors DONDAPATI SUNEEL VARMA, A TOSHIBA PRAVEEN KUMAR for their support.

My wholehearted gratitude to my parents, Mr. RAJKUMAR PRASAD and Mrs. URMILA DEVI and my brothers Mr. ANIL KUMAR and RAVI PRAKASH for their encouragement and support.

PAWAN KUMAR
Rourkela, MAY 2014

Contents

Contents	i
List of Figures	v
List of Tables	vii
1 Introduction	1
1.1 Introduction	1
1.2 Literature Review	1
1.3 Objective	2
1.4 Thesis Organisation	2
2 Antenna Array	4
2.1 Linear Antenna Array	4
2.1.1 Introduction	4
2.1.2 Array Factor of LAA	4
2.1.3 Properties of antenna arrays	7
2.2 Planar Antenna Array	9
2.2.1 Array Factor of PAA	9
2.3 Hexagonal Prism Array	10
2.3.1 Introduction	10
2.3.2 Array Factor Formulation Of HPA	11
3 Array Synthesis Using Bat Algorithm	16

3.1 Introduction	16
3.2 Bat Algorithm	16
3.3 Flow Chart of BA	18
3.4 Performance Comparision of Bat and PSO(Khodier) Applied to LAA	20
4 Simulation Results & Discussion	22
4.1 Introduction	22
4.2 Fitness Function	22
4.3 Optimisation of LAA by BA	24
4.3.1 Amplitude Excitation Optimisation of LAA	24
4.3.2 Complex Excitation Optimisation of LAA	25
4.3.3 Relative Distance Optimisation of LAA	27
4.4 Optimisation of PAA by BA	30
4.4.1 Amplitude Excitation Optimisation of PAA	30
4.4.2 Complex Excitation Optimisation of PAA	32
4.4.3 Relative Distance Optimisation in PAA	32
4.5 Optimisation of HPA by BA	35
4.5.1 Amplitude Excitation Optimisation of HPA	35
4.5.2 Complex Excitation Optimisation of HPA	35
4.5.3 Comparative Study of Various controlling parameters of HPA	40
4.6 Application	42
5 CST Implementation of HPA	43
5.1 CST Studio	43
5.1.1 CST Microwave Studio	43
5.1.2 Patch dipole	44
5.1.3 Implementation HPA in CST	46
5.1.4 Comparision Between CST and MATLAB	47
6 HPA Synthesis Using Graphical User Interface(GUI)	52
7 Conclusion And Future Scope	54

7.1 Conclusion	54
7.2 Limitations	54
7.3 Future Scope	55
Bibliography	56

Abstract

In this dissertation a new architecture of antenna array is proposed in which antenna elements are placed on a Hexagonal Prism in order to obtain split beam radiation pattern. The Hexagonal Prism Array (HPA) is synthesized for amplitude excitation, complex excitation and relative distance using a novel optimisation technique. As a performance criteria the split beam radiation pattern is evaluated for side lobe level (SLL) and half power beam width (HPBW). The optimisation technique is experimented on conventional arrays like Linear and Planar and a comparative study with the published literature is also performed. An attempt to model the HPA on a commercial software in which radiator is a patch elements.

List of Figures

2.1 Linear Antenna Array	5
2.2 Phaser diagram of LAA	5
2.3 Shifted Antenna Array	7
2.4 Shifted Antenna Array	8
2.5 Planar Antena Array	9
2.6 Geometry of HPA	11
2.7 Shifting and Rotation in Plane 1,2 and 3	14
2.8 Shifting and Rotation in Plane 4,5 and 6	15
3.1 Flow Chart Of BA	19
3.2 LAA placed symmetrically along x-axis	20
3.3 Comparision between BA and PSO(Khodier)	21
4.1 Desired Radiation Pattern	23
4.2 Simulation Results of LAA By Amplitude Excitation optimisation	26
4.3 Simulation Results of LAA By Complex Excitation optimisation .	28
4.4 Simulation Results of LAA By Relative Distance Optimisation . .	29
4.5 Simulation Results of PAA By Amplitude Excitation optimisation	31
4.6 Simulation Results of PAA By Complex Excitation optimisation .	33
4.7 Simulation Results of PAA By Relative Distance optimisation . . .	34
4.8 Simulation Results of HPA By Amplitude Excitation optimisation	36
4.9 Simulation Results of HPA By Complex Amplitude Excitation . .	38
4.10Simulation Results of HPA By Relative Distance optimisation . . .	39

4.11	Combined Simulation Results of HPA	41
4.12	Synthetic Aperture Radar	42
5.1	Patch Antenna	45
5.2	Geometric View of HPA Using CST Studio	47
5.3	3-D Radiation Pattern of HPA in CST	47
5.4	Radiation Pattern at $\phi=0$ in CST	48
5.5	Radiation Pattern at $\phi=0$ in MATLAB	48
5.6	Radiation Pattern at $\phi=90$ in CST	48
5.7	Radiation Pattern at $\phi=90$ in MATLAB	49
5.8	Radiation Pattern at $\theta=0$ in CST	49
5.9	Radiation Pattern at $\theta=90$ in CST	49
5.10	Polar Plot of HPA using CST	50
5.11	Return Loss in HPA	51
6.1	Simulation Results of HPA in GUI	53

List of Tables

3.1 Analogy Between Bat and Antenna	18
3.2 Comparison between BA an PSO (Khodier)	21
4.1 Constraint Used in Optimisation	24
4.2 SLL & HPBW in Amplitude Excitation Optimisation	25
4.3 SLL & HPBW in Complex Excitation Optimisation	27
4.4 SLL & HPBW in Relative Distance Optimisation	27
4.5 SLL & HPBW in Amplitude Excitation Optimisation	31
4.6 SLL & HPBW in Complex Excitation Optimisation	32
4.7 SLL & HPBW in Relative Distance Optimisation	33
4.8 SLL & HPBW by Amplitude excitation Optimisation	35
4.9 SLL & HPBW by Complex Excitation Optimisation	37
4.10SLL & HPBW by Relative Distance Optimisation	37
4.11Comarision of optimisation of different parameters of HPA	40
5.1 Parameters Used in Designing the Patch	45

List of Abbreviations

Abbreviation	Description
AF	Array Factor
LAA	Linear Antenna Array
PAA	Planar Antenna Array
HPA	Hexagonal Prism Array
BA	Bat Algorithm
SLL	Side Lobe Level
HPBW	Half Power Beam width
SAR	Synthetic Aperture Radar
CST	Computer Simulation Technique

Chapter 1

Introduction

1.1 Introduction

In communication system there is always need of high gain,sharp beam and reduced SLL.Conformal arrays proves better in increasing gain.In Hexagonal Prism Array(HPA) antenna elements are placed at hexagonal shape.Proper choice of various parameters(Excitation,Relative distance) of antenna array can lead to a various shaped beam patterns.Optimisation of controlling parameters can aim at resolving the radiation pattern.

1.2 Literature Review

Linear antenna array and planar antenna array are used to give sharp beam[1],[2].Later use of conformal array made a great change in antenna synthesis and used for 3-D radiation pattern [6].HPA works better to give desired radiation pattern.

For improving directivity,HPBW and SLL many approach like Schellkunoff method,Fourier Transform method,Woodward Lawson method,Binomial method,Dolph Tchebyscheff were used [3, 4, 5]. Requirement of the radiation pattern in certain direction or in multi directions lead to many optimisation algorithms such as Particle Swarms Optimization(PSO),Firefly Algorithm(FA),Invasive Weed Optimization(IWO),Differential algorithm,Tabu Search Optimisation(TSO)

[7, 8, 9, 10, 11, 12]. Bat Algorithm is another evolutionary technique in this regard developed by Yang in 2010 [13]. These techniques are also used in solving different engineering problems [14, 15, 16, 17].

In 1959 frequency independent split beam is generated by Du Hamel Raymond H and Ore Fred R [19]. In this thesis also split beam is generated. For this purpose HPA controlling parameters is optimised by BA. Split beam can be used in Synthetic Aperture Radar (SAR) [18].

1.3 Objective

- The aim of the work is to synthesize HPA.
- To generate a split beam by using HPA.
- For generating the split beam a novel Evolutionary Algorithm is used.
- Implementation of HPA using computer Simulation Technology (CST) and validation.

1.4 Thesis Organisation

- Chapter 2 is antenna arrays. In this chapter array factor of LAA and PAA is discussed and by using shifting and rotational property of arrays, Array Factor formulation of HPA is done.
- In chapter 3 Bat algorithm (BA) is discussed and also a comparative study for linear array with PSO (Khodier) is done for 16 elements.
- In chapter 4 simulation results of LAA, PAA and HPA is discussed. In this chapter Optimising parameters like amplitude excitation optimisation, complex distance optimisation and relative distance optimisation of LAA, PAA and HPA is done to give desired split beam.

- In chapter 5 HPA synthesis in CST is discussed and also its results are compared with simulation results of MATLAB. For synthesizing HPA patch dipoles are used.
- In chapter 6 HPA is discussed using GUI (Graphical User Interface). In this chapter GUI is used to give the radiation pattern, SLL and HPBW by putting the input value of parameters of BA and HPA.
- In chapter 7 conclusion and future works are discussed.

Chapter 2

Antenna Array

2.1 Linear Antenna Array

2.1.1 Introduction

A single antenna has a limited directivity, but in some advanced areas it is required to have a highly directional radiation pattern. Hence, with the use of antenna elements working together (array), it is possible to improve the radiation according to some desired specification.

2.1.2 Array Factor of LAA

Radiation pattern of single antenna element is relatively wide hence directive gain is low. Array of antennas is used to direct radiated power towards a desired angular sector. Hence directivity can be increased without increasing the size of antenna elements[5].

A linear array placed in z-direction element, has an omnidirectional pattern with respect to the azimuthal angle ϕ with each element has their individual radiation field as shown in figure 2.1. The total field of the array is equal to the field of a single element positioned at the origin multiplied by a factor which is widely referred to as the array factor. Phasor diagram of LAA is

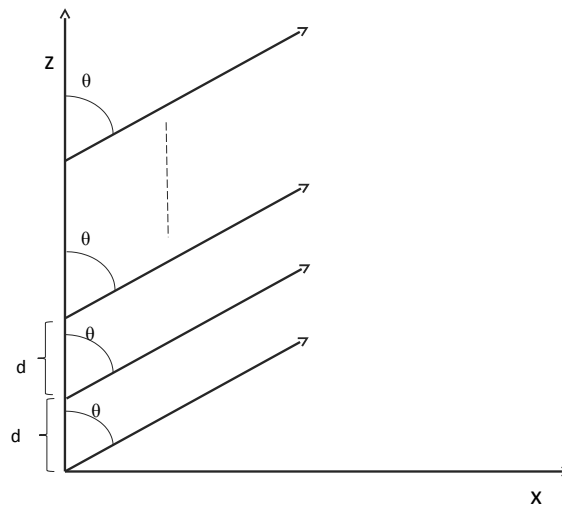


Figure 2.1: Linear Antenna Array

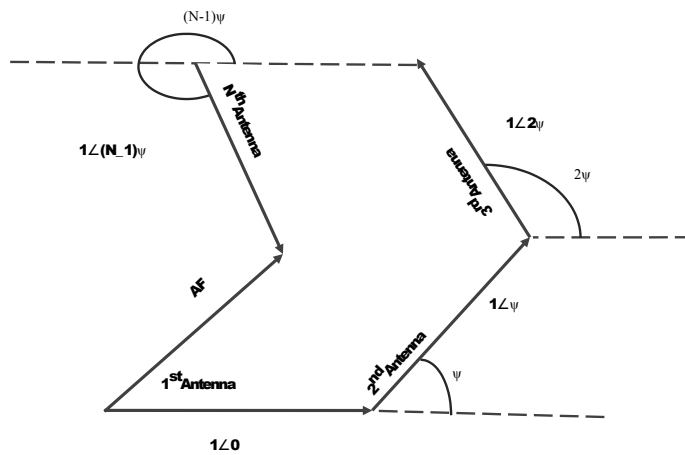


Figure 2.2: Phasor diagram of LAA

shown in Figure 2.2

Array factor(AF) of LAA can be calculated as[3, 1]

$$AF = I_0 + I_1 * e^{j\Psi} + I_2 * e^{j*2*\Psi} + \dots + I_{N-1} * e^{j*(N-1)\Psi}$$

$$AF = \sum_{n=0}^{N-1} I_n e^{j(n)\Psi} \tag{2.1}$$

where Ψ is the progressive phase shift, I_n is the current excitation N is the number of elements.

where $\Psi = kdcos\gamma + \beta$

Where k is free space wave number, d is the distance between the elements γ is the angle between axis of array and line from origin to observation point and can be obtained from the dot product of a unit vector along the axis of the array with a unit vector directed toward the observation point and β is difference in current phase excitation between the elements. If array is placed in z -direction as shown in Figure 2.1 then

$$cos\gamma = \hat{a}_z \cdot \hat{a}_r \quad (2.2)$$

$$cos\gamma = \hat{a}_z \cdot (\hat{a}_x \cdot sin\theta \cdot cos\phi + \hat{a}_y \cdot sin\theta \cdot sin\phi + \hat{a}_z \cdot cos\theta) \quad (2.3)$$

where ϕ is azimuthal angle and θ is the elevation angle.

$$cos\gamma = cos\theta$$

$$\gamma = \theta$$

$$\Psi = kdcos\theta + \beta$$

Hence array factor for z -direction is given as

$$AF_z = \sum_{n=0}^{N-1} I_n e^{jn(kdcos\theta + \beta)} \quad (2.4)$$

Similarly if array is placed in y -direction then

$cos\gamma = sin\theta \cdot sin\phi$ Hence array factor for y -direction is given as

$$AF_y = \sum_{n=0}^{N-1} I_n e^{jn(kdsin\theta \cdot sin\phi + \beta)} \quad (2.5)$$

Similarly if array is placed in x -direction then

$cos\gamma = sin\theta \cdot cos\phi$ Hence array factor for x -direction is given as

$$AF_x = \sum_{n=0}^{N-1} I_n e^{jn(kdsin\theta \cdot cos\phi + \beta)} \quad (2.6)$$

If $k_x = kdsin\theta \cdot cos\phi + \beta$, $k_y = kdsin\theta \cdot sin\phi + \beta$ and $k_z = kdcos\theta + \beta$, then array factor in x, y & z -direction is given as [2]

$$AF_x = \sum_{n=0}^{N-1} I_n e^{jnk_x d} \quad (2.7)$$

$$AF_y = \sum_{n=0}^{N-1} I_n e^{jnk_y d} \quad (2.8)$$

$$AF_z = \sum_{n=0}^{N-1} I_n e^{jnk_z d} \quad (2.9)$$

where k_x, k_y & k_z are wave number in x,y and z-direction respectively. In General it can be said that

$$AF_\gamma = \sum_{n=0}^{N-1} I_n e^{jnk_\gamma d} \quad (2.10)$$

from equation 2.10 and it can be said that

$$\Psi = k_\gamma * d \quad (2.11)$$

2.1.3 Properties of antenna arrays

Shifting Property

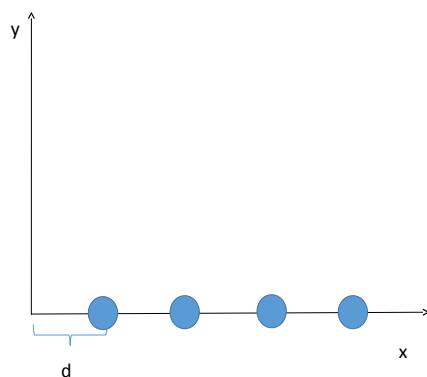


Figure 2.3: Shifted Antenna Array

If antenna array is not placed at origin and start with distance ‘d’ from origin as shown in Figure 2.3 then array factor is given as:

$$\begin{aligned}
AF_s &= I_0 * e^{j\Psi} + I_1 * e^{j2\Psi} + I_2 * e^{j3\Psi} + \dots + I_{N-1} * e^{j(N)\Psi} \\
AF_s &= e^{j\Psi}(I_0 + I_1 * e^{j\Psi} + I_2 * e^{j2\Psi} + \dots + I_{N-1} * e^{j(N-1)\Psi}) \\
AF_s &= e^{j\Psi} * AF
\end{aligned} \tag{2.12}$$

From equation 2.11

$$AF_s = e^{jk_\gamma d} * AF \tag{2.13}$$

If any type of array is shifted by 'd' distance in γ direction then array factor of shifted array [2] is given by equation 2.13

Rotational Property

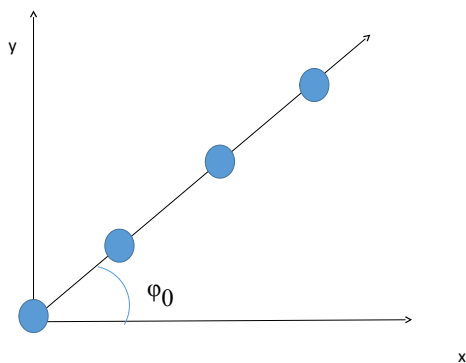


Figure 2.4: Shifted Antenna Array

If antenna array is placed at angle ϕ_0 with respect to x-axis as shown in Figure 2.4 then

$$\cos\gamma = (\hat{a}_x \cdot \cos\phi_0 + \hat{a}_y \cdot \sin\phi_0) \cdot (\hat{a}_x \cdot \sin\theta \cdot \cos\phi + \hat{a}_y \cdot \sin\theta \cdot \sin\phi + \hat{a}_z \cdot \cos\theta) \tag{2.14}$$

$$\cos\gamma = \cos\phi_0 \cdot \sin\theta \cdot \cos\phi + \sin\phi_0 \cdot \sin\theta \cdot \sin\phi$$

$$\cos\gamma = \sin\theta \cdot \cos(\phi - \phi_0) \tag{2.15}$$

$$AF_r = \sum_{n=0}^{N-1} I_n e^{jn[kd \sin\theta \cdot \cos(\phi - \phi_0) + \beta]} \tag{2.16}$$

From equation 2.6 and 2.16 if array factor in x-direction is represented as $AF_x(\theta, \phi)$ and array is rotated with angle ϕ_0 towards y-direction then array factor of rotated array is

$$AF_r = AF_x(\theta, (\phi - \phi_0)) \quad (2.17)$$

Similarly if array factor in y-direction is represented as $AF_y(\theta, \phi)$ and array is rotated with angle δ_0 towards x-direction then array factor of rotated array is given as

$$AF_r = AF_y(\theta, (\phi + \delta_0)) \quad (2.18)$$

2.2 Planar Antenna Array

LAA produces a reduced side lobe level(SLL),provides sharp beam-width and improves directivity.but the disadvantage of LAA is its large size and not radiating in a particular direction.It is very difficult to use linear array for 3-D space.Another way to improve directivity is to increase the elements in a plane rather than in an axis.This modification in the geometry leading to Planar Antenna Array(PAA).PAA is combination of linear arrays.It is shown in Figure 2.5.Size of PAA is less than LAA which is an advantage.PAA also improves HPBW and reduces SLL.

2.2.1 Array Factor of PAA

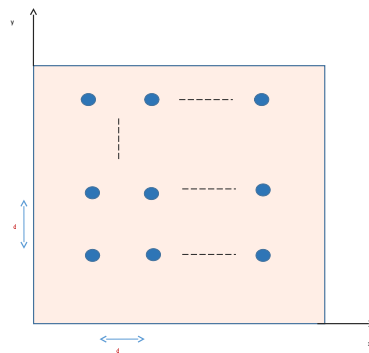


Figure 2.5: Planar Antenna Array

For calculation of array factor of PAA(AF_p) it can be said that it is a combination of shifted version of linear arrays. If array factor in x-direction is given as AF_x . Then by using shifting property of linear array from equation 2.13 and combining them array factor can be given as

$$AF_p = AF_x + AF_x * e^{jk_y*d} + AF_x * e^{jk_y*2d} + AF_x * e^{jk_y*3d} + \dots AF_x * e^{jk_y*(M-1)d}$$

$$AF_p = AF_x(1 + e^{jk_y*d} + e^{jk_y*2d} + e^{jk_y*3d} + \dots e^{jk_y*(M-1)d})$$

$$AF_p = AF_x * \sum_{m=0}^{M-1} * e^{jmkyd}$$

$$AF_p = AF_x * AF_y$$

If PAA is placed in x-z plane then array factor is given as

$$AF_{xz} = AF_x * AF_z$$

If all antenna elements have different current excitation then array factor of PAA placed in x-y plane is given as

$$AF_{xy} = \sum_{n=0}^{N-1} \sum_{m=0}^{M-1} I_{mn} e^{jnk_xd} * e^{jmkyd} \quad (2.19)$$

2.3 Hexagonal Prism Array

2.3.1 Introduction

Hexagonal Prism Array (HPA) is combination of six planar arrays whose first plane is placed in x-z plane and then each plane is rotated 120° with previous one. Due to this reason it provide omnidirectional pattern. Also by optimising the controlling parameters of HPA it is possible to get desired radiation pattern in particular direction without rotation of whole array. By using HPA it is possible to increase directivity, reduced SLL and sharper beam which can be applicable in satellite and radar communication.

2.3.2 Array Factor Formulation Of HPA

Array Factor of HPA is combination of array factor of six planar arrays. For calculating array factor of HPA shifting and rotational property is used as discussed in section 2.1.3. Geometry of HPA in 3-D view is shown in Figure 2.6a and corresponding top view is shown in Figure 2.6b. From the Figure 2.6a it can be seen that plane is rotating and shifting in xy plane and constant with respect to z-axis. Hence array factor with respect to z-axis is constant for every plane. From figure 2.6b shifting distance for each plane from origin means d_1, d_2, d_3, d_4 and d_5 can be calculated in terms of distance between the elements 'd'

Here $d_1 = (N + 1)d$, $d_2 = (N + 1)\sqrt{3}d$, $d_3 = (N + 1)2d$, $d_4 = (N + 1)\sqrt{3}d$ and $d_5 = (N + 1)d$ where N is the number of elements in x-direction in one row. Rotation and Shifting Of each plane is shown in Figure 2.7 and 2.8.

First plane is placed in x-z plane hence. Hence its array factor is given by equation 2.20.

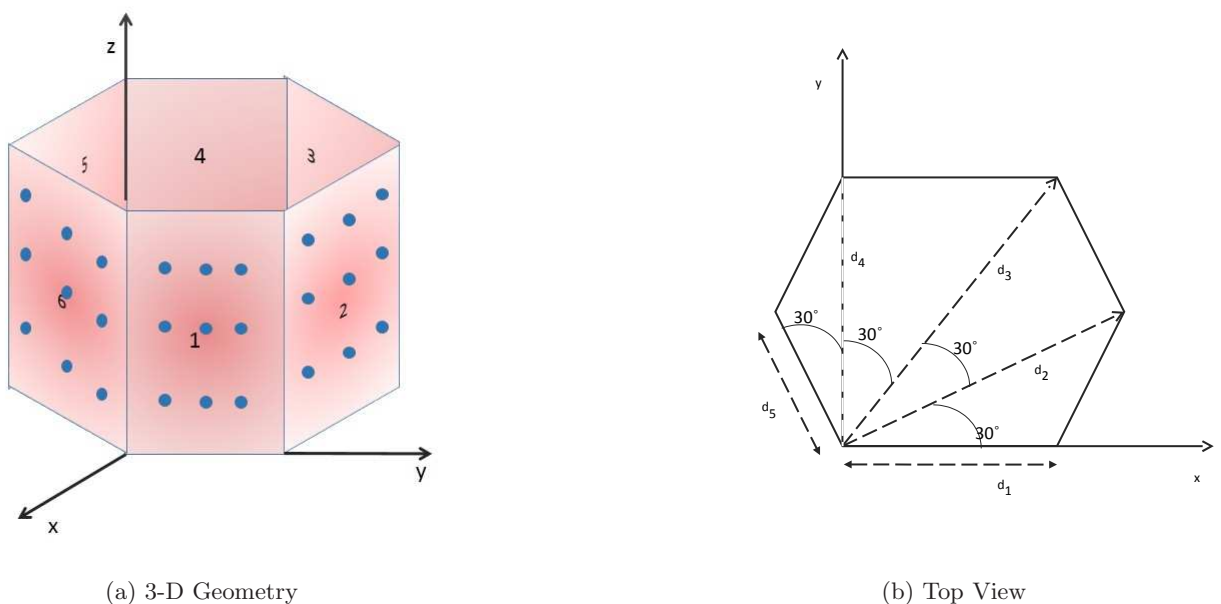


Figure 2.6: Geometry of HPA

$$AF_1 = \sum_{n=1}^N \sum_{m=1}^M \left[I_{mn} * e^{(j(n-1)kdsin\theta cos\phi)} \right] * \left[e^{(j(m-1)k_z d)} \right] \quad (2.20)$$

Here N is the number of elements in x-direction and M is the number of elements in z-direction and I_{mn} is the current excitation of each element in the plane. For calculation of array factor of second plane it can be seen from Figure 2.7c that it is first rotated with angle 60° with respect to x-axis and then it is shifted with distance ' d_1 '. Hence by using rotational property discussed in equation 2.17 array factor of plane '2' after rotation is given by equation 2.21.

$$AF_{r2} = \sum_{n=1}^N \sum_{m=1}^M \left[I_{mn} * e^{(j(n-1)kdsin\theta\cos(\phi-\pi/3))} \right] * \left[e^{(j(m-1)k_zd)} \right] \quad (2.21)$$

after that it is shifted by distance d_1 Hence by using shifting property from equation 2.13 array factor of plane '2' is given as equation 2.22

$$AF_2 = AF_{r2} e^{jk_x d_1}$$

$$AF_2 = \sum_{n=1}^N \sum_{m=1}^M \left[I_{mn} * e^{(j(n-1)kdsin\theta\cos(\phi-\pi/3))} \right] * \left[e^{(j(m-1)k_zd)} \right] * \left[e^{jk_x d_1} \right] \quad (2.22)$$

Similarly plane 3 is rotated 120° . Hence array factor of rotated array of plane 3 is given as

$$AF_{r3} = \sum_{n=1}^N \sum_{m=1}^M \left[I_{mn} * e^{(j(n-1)kdsin\theta\cos(\phi-2\pi/3))} \right] * \left[e^{(j(m-1)k_zd)} \right] \quad (2.23)$$

then it is shifted ' d_2 ' distance in the direction of 30° from x-axis. Hence here

$$k_\gamma = k_x \cos\pi/6 + k_y \sin\pi/6$$

By using shifting property from equation 2.13 array factor of plane '3' is given as equation 2.24

$$AF_3 = AF_{r3} * \left[e^{(j(k_x \cos\pi/6 + k_y \sin\pi/6)d_2)} \right]$$

$$AF_3 = \sum_{n=1}^N \sum_{m=1}^M \left[I_{mn} * e^{(j(n-1)kdsin\theta\cos(\phi-2*\pi/3))} \right] * \left[e^{(j(m-1)k_zd)} \right] * \left[e^{(jk_x\cos\pi/6+k_y\sin\pi/6)d_2} \right] \quad (2.24)$$

Similarly array factor of successive planes is given by equations 2.25,2.26 and 2.27 respectively.

$$AF_4 = \sum_{n=1}^N \sum_{m=1}^M \left[I_{mn} * e^{(j(n-1)kdsin\theta\cos(\phi-\pi))} \right] * \left[e^{(j(m-1)k_zd)} \right] * \left[e^{(j(k_x\cos2*\pi/6+k_y\sin2*\pi/6)d_3)} \right] \quad (2.25)$$

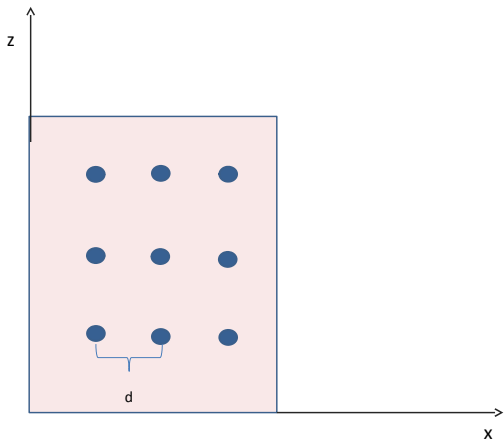
$$AF_5 = \sum_{n=1}^N \sum_{m=1}^M \left[I_{mn} * e^{(j(n-1)kdsin\theta\cos(\phi-4\pi/3))} \right] * \left[e^{(j(m-1)k_zd)} \right] * \left[e^{(j(k_x\cos3*\pi/6+k_y\sin3*\pi/6)d_4)} \right] \quad (2.26)$$

$$AF_6 = \sum_{n=1}^N \sum_{m=1}^M \left[I_{mn} * e^{(j(n-1)kdsin\theta\cos(\phi-5\pi/3))} \right] * \left[e^{(j(m-1)k_zd)} \right] * \left[e^{(j(k_x\cos4\pi/6+k_y\sin4\pi/6)d_5)} \right] \quad (2.27)$$

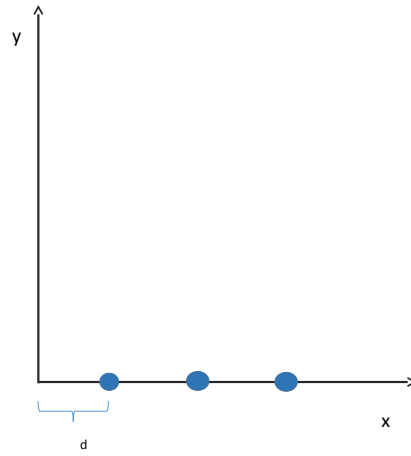
Finally total array factor is summation of all six planar array and it is given by equation 2.28.

$$AF_{Hex} = \sum_{p=0}^5 \sum_{n=1}^N \sum_{m=1}^M \left[I_{mnp} * e^{(j(n-1)kdsin\theta\cos(\phi-(p-1)\pi/3))} \right] * \left[e^{(j(m-1)k_zd)} \right] * \left[e^{(j(k_x\cos(p-1)\pi/6+k_y\sin(p-1)\pi/6)d_{(p)})} \right] \quad (2.28)$$

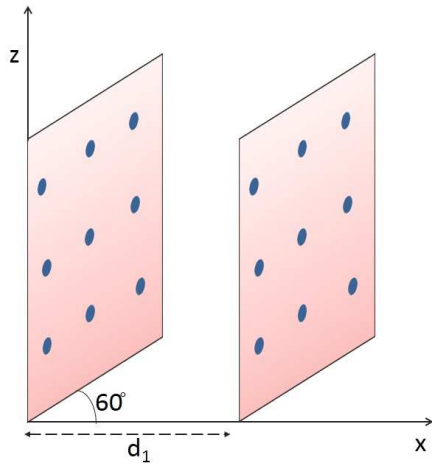
Here p is $(p+1)^{th}$ plane of HPA. In this way array factor of HPA is calculated.



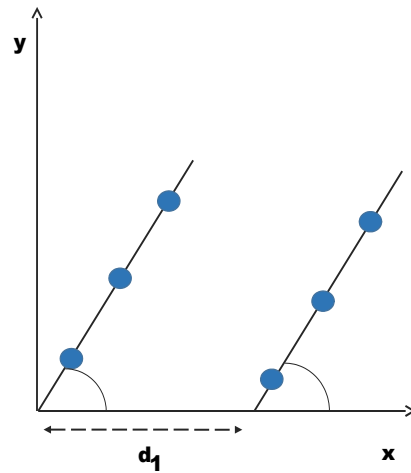
(a) Side View of plane 1



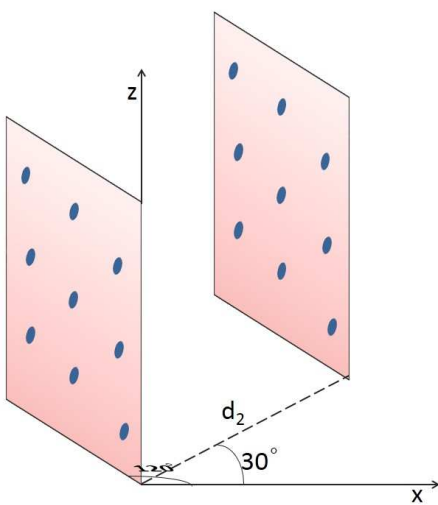
(b) Top View of plane 1



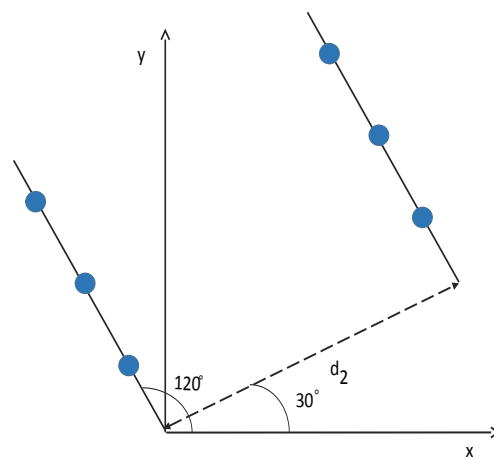
(c) Side View of plane 2



(d) Top View of plane 3

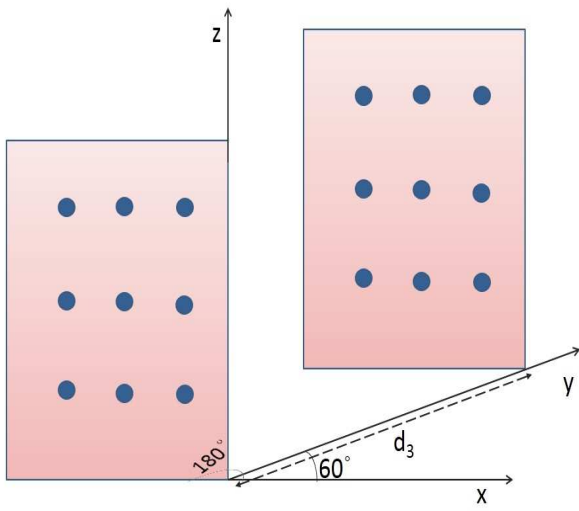


(e) Side View of plane 3

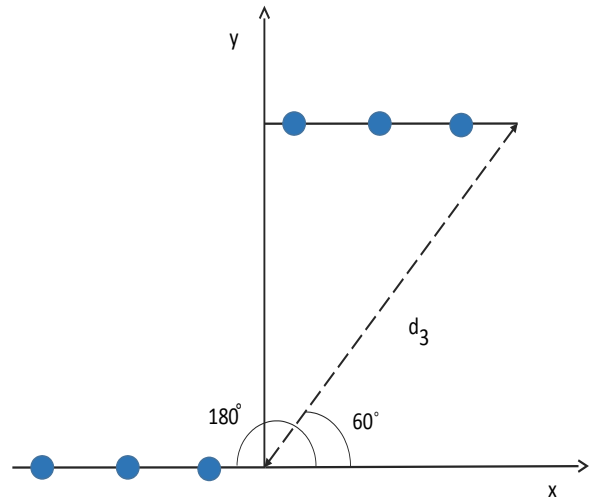


(f) Top View of plane 3

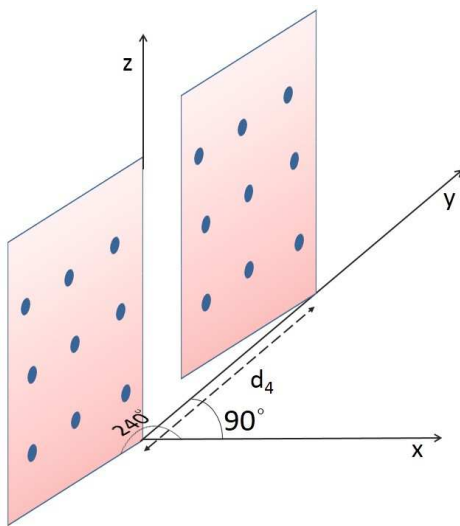
Figure 2.7: Shifting and Rotation in Plane 1,2 and 3



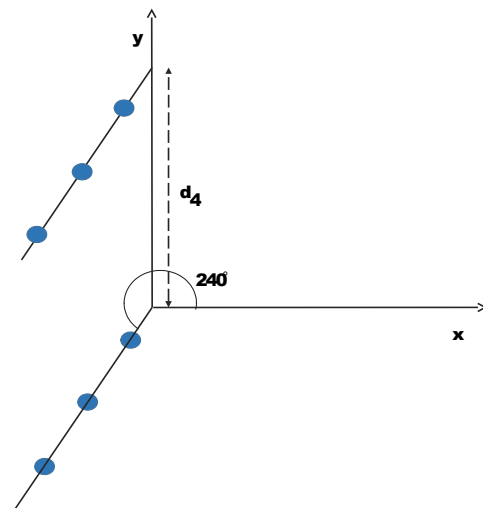
(a) Side View of plane 4



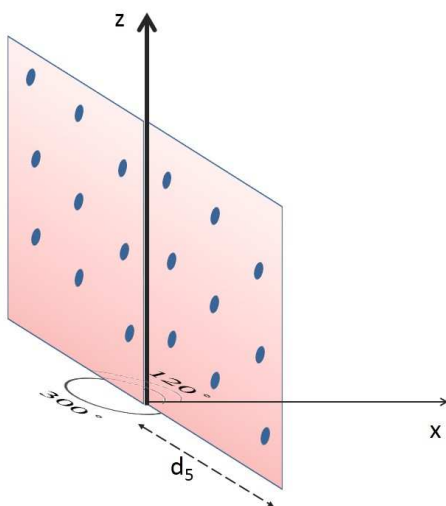
(b) Top View of plane 4



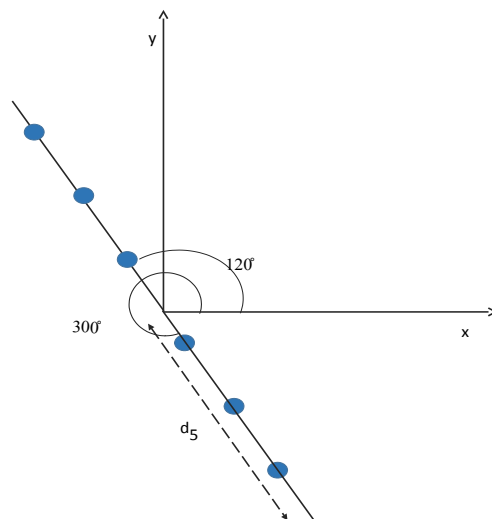
(c) Side View of plane 5



(d) Top View of plane 5



(e) Side View of plane 6



(f) Top View of plane 6

Figure 2.8: Shifting and Rotation in Plane 4,5 and 6

Chapter 3

Array Synthesis Using Bat Algorithm

3.1 Introduction

Antenna array synthesis using nature inspired algorithm is used to get the desired radiation pattern. Earlier many traditional approach like Schellkunoff method, Fourier Transform method, Woodward Lawson method, Binomial method, Dolph Tchebyscheff method and so on were used for beam shaping and null placement in antenna array synthesis. But these days evolutionary algorithms like Particle Swarms Optimization (PSO), Firefly Algorithm (FA), Invasive Weed Optimization (IWO), Differential algorithm, Tabu Search Optimisation (TSO) and Bat algorithm (BA) are used for different optimisation. [9, 10, 11, 12]. Bat Algorithm is another approach in optimisation developed by Yang in 2010 [13]. BA is also developed for multi-objective function. [15, 14, 16]. These techniques are also being used in antenna synthesis [7], [8].

3.2 Bat Algorithm

BA is based on echolocation behaviour of bats. By using echolocation bats are able to find their food/prey. This technique can be used to solve various engineering problems. Teodoro C. Bora used BA for solving DC Wheel Motor Problem [17].

In this thesis BA is used for optimizing the different controlling parameters of antenna arrays like amplitude excitation, relative distance optimization and complex amplitude excitation to give desired pattern.

In this algorithm some basic rules were used which is discussed following:

1. Bats works on the principle of echolocation to sense distance.
2. To find the prey bats flying randomly with velocity v_i at position x_i , frequency can be tuned from f_{min} to f_{max} , Wavelength of their emitted pulses and rate of pulse emission r is adjusted in the range of $[0,1]$, depending on the proximity of their target;
3. It is assumed that the loudness is varied from a large (positive) A_0 to a minimum constant value A_{min} .

As iteration increases position x_i^t and velocities v_i^t at time step t are updated according to the following equation:

$$f_i = f_{min} + (f_{max} - f_{min})\beta \quad (3.1)$$

$$v_i^t = v_i^{t-1} + (x_i^t - x_*)f_i \quad (3.2)$$

$$x_i^t = x_i^{t-1} + v_i^t \quad (3.3)$$

where $\beta \in [0, 1]$ shows a random vector drawn from a uniform distribution. In this algorithm the current global best location (solution) is denoted by x_* which is located after comparing all the solutions among all the n bats.

After each iteration once a solution is selected among the current best solutions, a new solution for each bat is generated locally using random walk:

$$x_{new} = x_{old} + \epsilon A^t \quad (3.4)$$

where $\epsilon \in [1, 1]$ represent a random number, while $A^t = \langle A_i^t \rangle$ shows the average loudness of all the bats at this time step.

In this work for antenna synthesis using BA $\epsilon = 0.1$ is used. As the iteration increases, the loudness A_i and the rate r_i of pulse emission have to be updated

according to the following formula:

$$A_i^{t+1} = \alpha A_i^t \quad (3.5)$$

$$r_i^{t+1} = r_i^t * (1 - \exp(-\gamma * t)) \quad (3.6)$$

where α and γ is constant. Generally $0 \leq \alpha \leq 1$ and $\gamma > 0$. In this thesis α is taken as 0.1 and γ is taken as 1.

Loudness decreases and pulse rate increases as iteration increases. If $A_{min} = 0$ means bat has just found the prey. Then it stop emitting pulses.

3.3 Flow Chart of BA

Steps of algorithm is discussed in flow chart 3.1. In the flow chart x_* is the current global best location located after comparing all the solutions among all the bats. Analogy in terms of Bat and Antenna is given in Table 3.1. Here two parameter loudness and pulse rate play an important role in optimising the controlling parameter of arrays. In each iteration loudness decreases and pulse rate increases. In this way in each iteration possible to reach the closer value of desired pattern.

Bats	Antenna
Bat locations	Solutions(Excitation,Relative Distance)
Bat population	Number of Solution
Best bat is selected	Best solution is selected
Local solution Generated by random walk	Local solution generated by step size
Prey is find	Desired Pattern is obtained

Table 3.1: Analogy Between Bat and Antenna

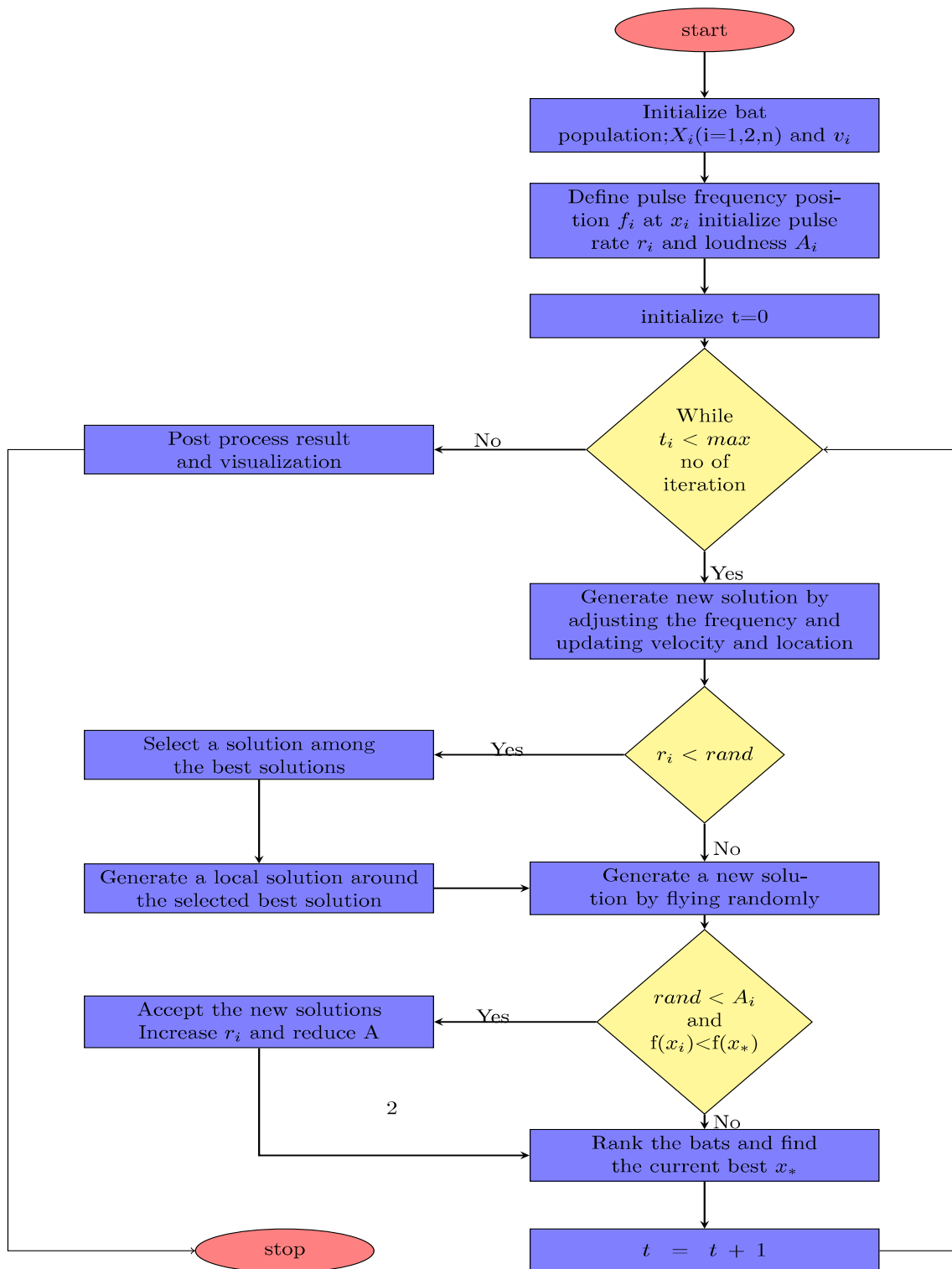


Figure 3.1: Flow Chart Of BA

3.4 Performance Comparison of Bat and PSO(Khodier) Applied to LAA

In this section result of BA is compared with PSO(Khodier). In this paper [8] elements are placed symmetrically along x-axis as shown in Figure 3.2. Fitness function is given as [8].

$$fitness = \min(\max\{20\log|AF(\phi)|\})$$

subject to $\phi \in \{[0^0, 76^0] \& [104^0, 108^0]\}$ Hence the aim is to minimized the maximum SLL. Radiation pattern which is shown in figure 3.3a for sixteen elements optimised for amplitude excitation. It can be seen that in the case of BA SLL is -44.27 dB which is -30.7dB in the case of published PSO result. This result shows BA is performing better for compared to PSO for given fitness function while constraint is SLL. Figure 3.3b shows amplitude distribution(normalised value) of two algorithms[8].

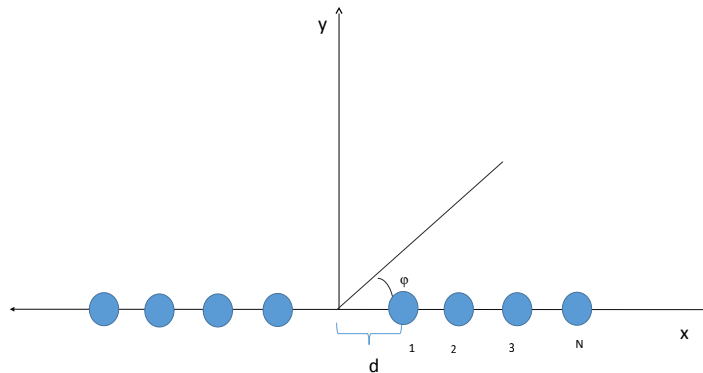
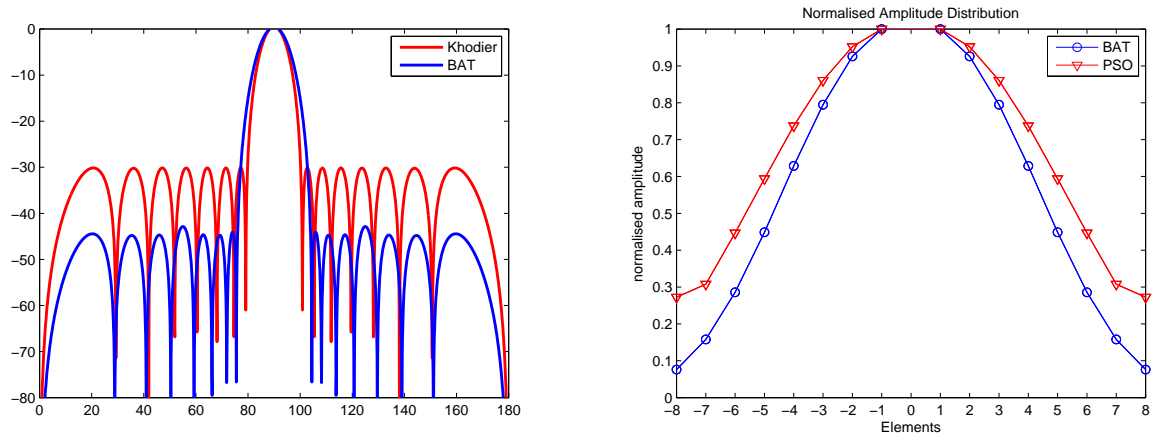


Figure 3.2: LAA placed symmetrically along x-axis

From Figure 3.3a it can be seen that SLL decreases but HPBW increases but LAA is optimum in terms of beamwidth. So difference between two is not more.



(a) Radiation Pattern Comparison

(b) Normalized amplitude distribution $|I_n|$ of array elements(Khodier)

Figure 3.3: Comparison between BA and PSO(Khodier)

	Amplitude(I_n)	SLL
PSO(Khodier)	1.0000,0.9521,0.8605,0.7372, 0.5940,0.4465,0.3079,0.2724	-30.7
BA	1.0000,0.9258,0.7948,0.6285, 0.4487,0.2857,0.1577,0.0762	-44.27

Table 3.2: Comparison between BA an PSO (Khodier)

Chapter 4

Simulation Results & Discussion

4.1 Introduction

In this chapter LAA,PAA and HPA synthesis is discussed which is used to give split beam.For this purpose controlling parameters of antenna is optimised by BA.To get split beam appropriate fitness function is adapted.A comparative study has also be done among LAA,PAA and HPA for desired pattern.

4.2 Fitness Function

The aim of this thesis is to get split beam with respect to elevation angle. Here this work is experimented by LAA,PAA and HPA. Desired radiation pattern is shown in Figure 4.1 For desired pattern there should be two main beam at $(-20^0 < \theta < -1^0)$ and $(1^0 < \theta < 20^0)$,one null of -20 dB at $(-1^0 \leq \theta \leq 1^0)$ and two nulls of -40 dB at $(-24^0 < \theta < -20^0)$ and $(20^0 < \theta < 24^0)$ and SLL at $(-180^0 \leq \theta \leq -24^0)$ and $(24^0 \leq \theta \leq 180^0)$. ϕ is constant as 0^0 for this case.

If desired array factor is f_d and optimised array factor is f_o then $f = f_o - f_d$ has to minimized.f denote difference between optimised and desired array factor. f_{MLL} , f_{SLL} , f_{null_1} , f_{null_2} denotes ‘main lobe level difference’,‘side lobe level difference’,‘difference of nulls of -40 dB’ and ‘difference of nulls of-20 dB’ of desired pattern and optimised pattern respectively. Hence fitness function

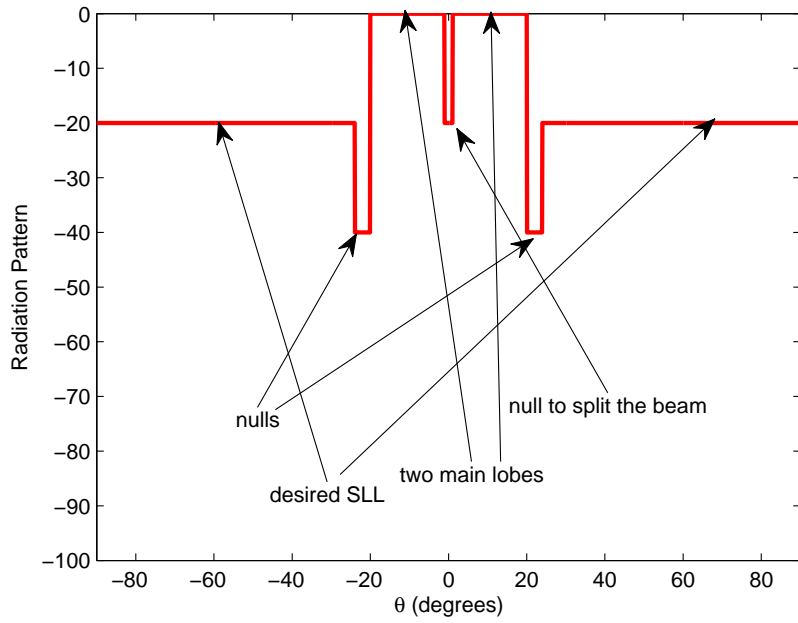


Figure 4.1: Desired Radiation Pattern

is given as

$$\begin{aligned}
 f_{MLL} &\in (-20^0 < \theta < -1^0) \text{ and } (1^0 < \theta < 20^0) \\
 f_{SLL} &\in (-180^0 \leq \theta \leq -24^0) \text{ and } (24^0 \leq \theta \leq 180^0) \\
 f_{null_1} &\in (-24^0 < \theta < -20^0) \text{ and } (20^0 < \theta < 24^0) \\
 f_{null_2} &\in (-1^0 \leq \theta \leq -1^0)
 \end{aligned}$$

$$\begin{aligned}
 fitness = \min(\alpha_1 * mean(|f_{SLL}|) + \alpha_2 * mean(|f_{MLL}|) + \alpha_3 * \\
 mean(|f_{null_1}|) + \alpha_4 * mean(|f_{null_2}|))
 \end{aligned}$$

Here $\alpha_1 = 0.3, \alpha_2 = 0.3, \alpha_3 = 0.15$ and $\alpha_4 = 0.25$

To achieve the desired pattern arrays are synthesised in three different ways with each time giving importance to one parameter :

1. Amplitude Excitation Optimisation
2. Complex Excitation Optimisation
3. Relative Distance Optimisation.

Iteration	1000
Population	200
Best Run	10

Table 4.1: Constraint Used in Optimisation

Array factor is function of excitation(I_n), distance from origin(d), elevation angle(θ), azimuthal angle(ϕ). I_n is complex parameter and contains two parts amplitude and phase. In ‘amplitude excitation optimisation’ amplitude of current excitation is optimised by BA [13], in ‘complex excitation optimisation’ complex value of current excitation (I_n) is optimised while all other parameters is kept constant and in ‘relative distance optimisation’ distance from origin to antenna elements(d) is optimised and other parameters will remain constant.

LAA, PAA and HPA are optimised using BA as discussed in chapter 3. In optimisation values of parameters is shown in Table 4.1.

4.3 Optimisation of LAA by BA

LAA controlling parameters are optimised using BA to give desired split beam. Antenna array is placed at y-axis. Array factor for antenna array placed in y-axis is discussed in section 2.8.

4.3.1 Amplitude Excitation Optimisation of LAA

In ‘amplitude excitation optimisation’, distance between elements is fixed as $\lambda/2$ for different configuration. The choice of current excitation phase(β) plays an important role in getting the split beam. Here two main beam is required one where θ lies between -20° and 1° and other between 20° and 1° . Hence peak value should be at -10° and 10° . Hence array factor after steering is given as

$$AF_y(\theta) = \sum_{n=0}^{N-1} I_n e^{(jnkdsin\theta \cdot sin\phi - (-1)^n * sin(10 * \pi / 180))} \quad (4.1)$$

No of elements	HPBW(Degree)	SLL(dB)
10	9.5	-5.133
30	4.8	-7.771
72	1.6	-6.183

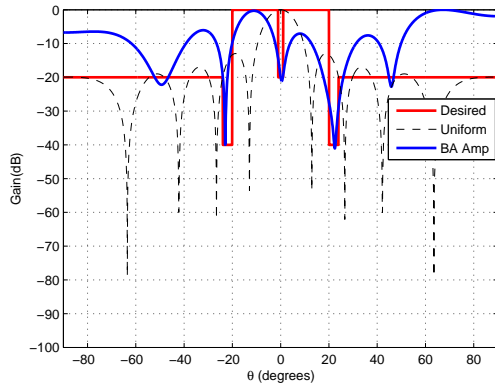
Table 4.2: SLL & HPBW in Amplitude Excitation Optimisation

Here ϕ is constant as $\pi/2$. Simulation results of amplitude excitation optimisation of LAA is shown in Figure 4.2. Radiation Pattern of 10 elements is shown in Figure 4.2a, For 30 elements shown in Figure 4.2c and for 72 elements shown in Figure 4.2e and their cost function is shown in Figure 4.2b, 4.2d and 4.2f respectively.

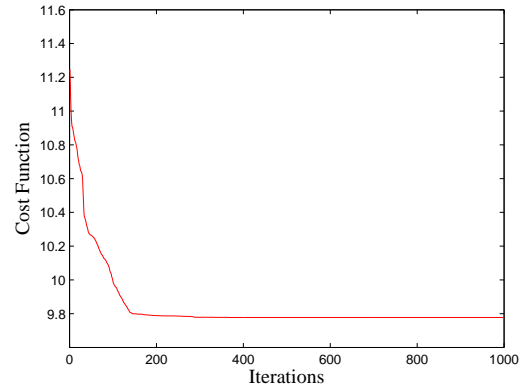
From Figure 4.2a and 4.2c it can be seen that for ‘10’ elements and for 30 elements only one main beam can be obtained. Hence in this case split beam is not obtained properly. In Figure 4.2e for 72 elements two main beams are obtained but two grating lobes are also there. HPBW and SLL is shown in table 4.2. From the table it can be seen that as number of elements increases HPBW decreases but SLL is not decreases upto the mark for large number of elements. From Figure 4.2b, 4.2d and 4.2f it can be seen that convergence rate for 72 elements is better compared 10 and 30 elements.

4.3.2 Complex Excitation Optimisation of LAA

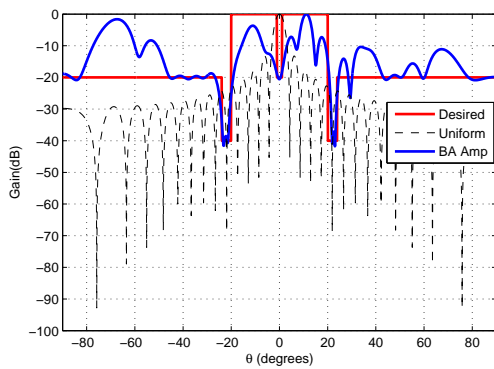
In this case complex value of current excitation is optimised by BA. Radiation pattern for 10, 30 & 72 elements is shown in Figure 4.3a, 4.3c & 4.3e and correspondingly their cost function is shown in Figure 4.3b, 4.3d & 4.3f. Here also can be seen that for 10 and 13 elements optimised pattern has only one main beam and for 72 elements two main beams are obtained means split beam is obtained but two grating lobes are coming into the picture. Its characteristics is shown in Table 4.3. From the table it can be seen that SLL reduction is better compared to amplitude excitation optimisation as discussed in Section 4.3.1. From cost function diagram it can be seen that convergence rate is better for 30 elements. Convergence rate ‘complex excitation optimisation’ is



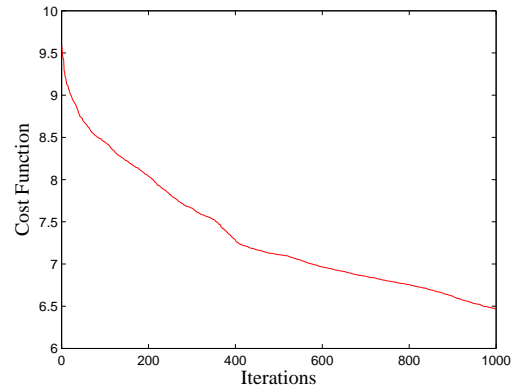
(a) Radiation Pattern for 10 elements



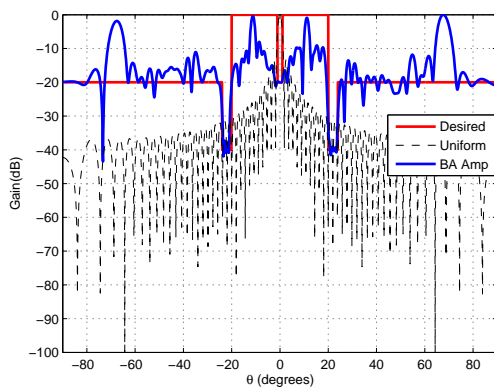
(b) Cost Function for 10 elements



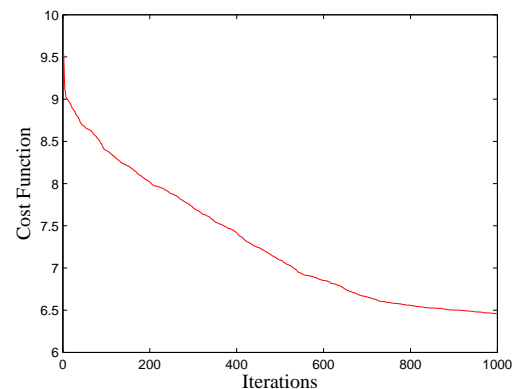
(c) Radiation Pattern for 30 elements



(d) Cost Function for 30 elements



(e) Radiation Pattern for 72 elements



(f) Cost Function for 72 elements

Figure 4.2: Simulation Results of LAA By Amplitude Excitation optimisation

No of elements	HPBW(Degree)	SLL(dB)
10	9.6	-17.71
30	4.9	-16.54
72	1.6	-8.72

Table 4.3: SLL & HPBW in Complex Excitation Optimisation

No of elements	HPBW(Degree)	SLL(dB)
10	6.7	-12.02
30	6.285	-16.23
72	8.15	-18.86

Table 4.4: SLL & HPBW in Relative Distance Optimisation

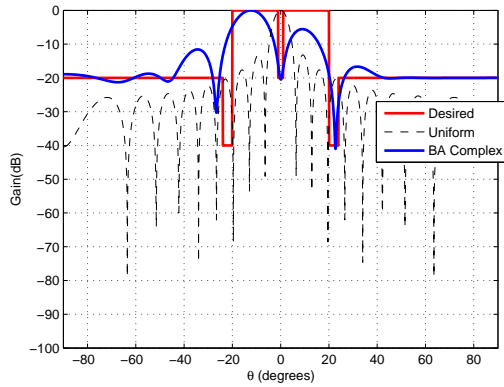
better than ‘amplitude excitation optimisation’ for same number of elements.

4.3.3 Relative Distance Optimisation of LAA

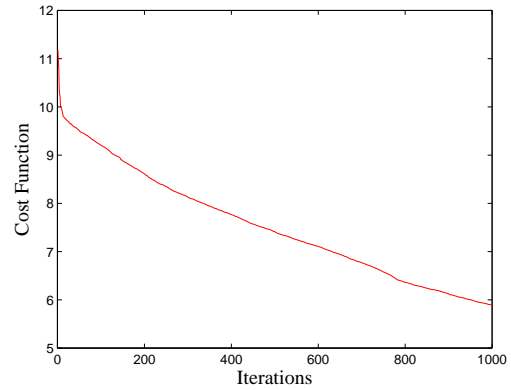
In relative distance optimisation elements are placed at non-uniform distance to give the desired pattern and value of these optimised distance is obtained by BA.

But array size should not increase than $number\ of\ elements \times \lambda/2$

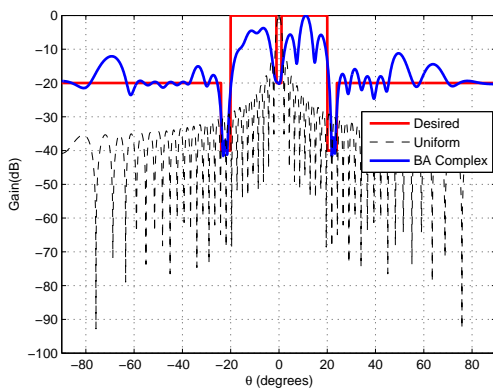
Radiation pattern for relative distance optimised LAA is shown in Figure 4.4a,4.4c & 4.4e and subsequently their cost function is shown in Figure 4.4b,4.4d & 4.4f. Its performance is shown in Table 4.4. From the figures it can be seen that relative distance optimisation works better for all three cases having two main beams. From the table it can be seen that SLL reduction is also better than amplitude excitation and complex amplitude optimisation. Average of HPBW is shown in Table 4.4. Due to asymmetric pattern nulls between main lobe is also not placed at $(-1^0 \leq \theta \leq 1^0)$ which is desired. For 10 elements null is placed at $\theta = -2.3^0$, for 30 elements it is placed at $(-1^0 \leq \theta \leq 1^0)$ but its value is -14.56 dB but desired value is -20 dB. For 72 elements it is placed at $(-1^0 \leq \theta \leq 1^0)$ and having value of -20 dB but it is unable to get another two nulls which should be at $(-24^0 < \theta < -20^0)$ and $(20^0 < \theta < 24^0)$.



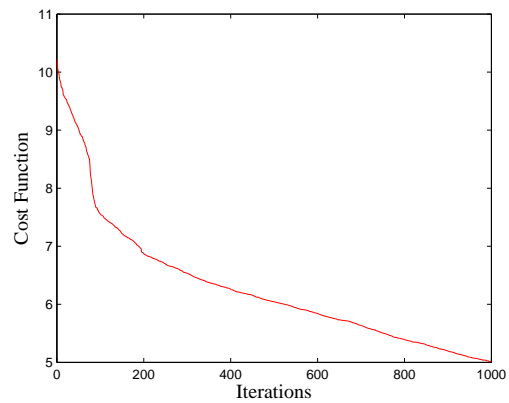
(a) Radiation Pattern for 10 elements



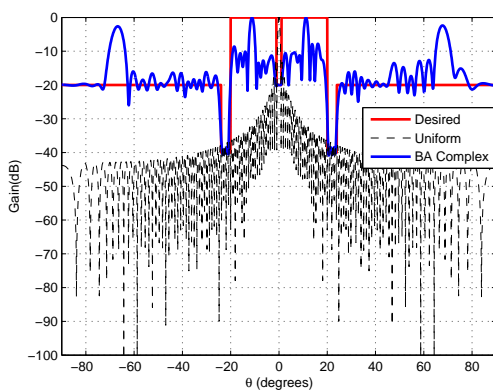
(b) Cost Function for 10 elements



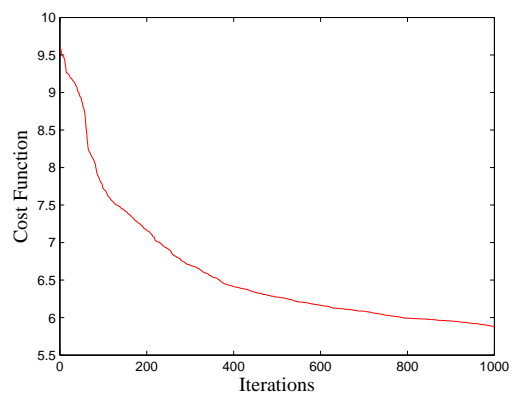
(c) Radiation Pattern for 30 elements



(d) Cost Function for 30 elements

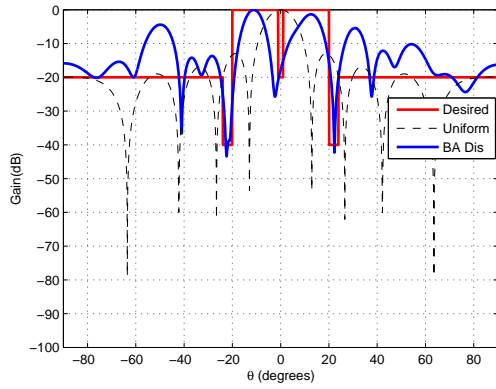


(e) Radiation Pattern for 72 elements

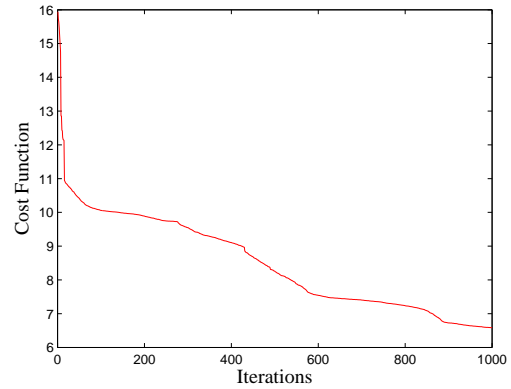


(f) Cost Function for 72 elements

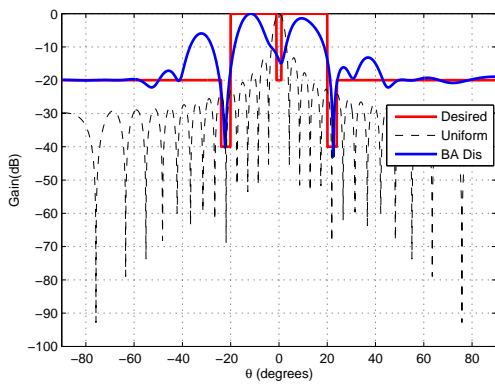
Figure 4.3: Simulation Results of LAA By Complex Excitation optimisation



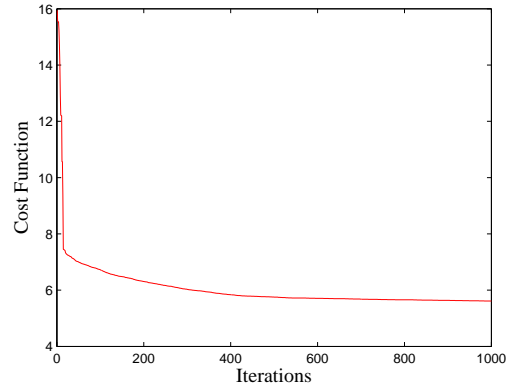
(a) Radiation Pattern for 10 elements



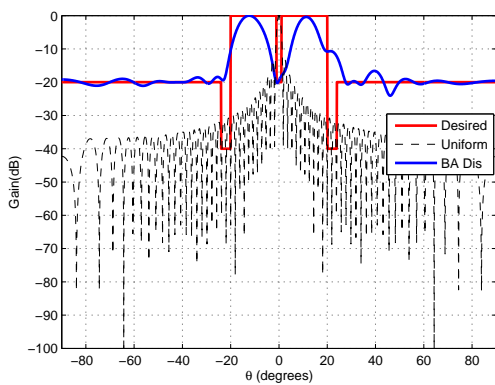
(b) Cost Function for 10 elements



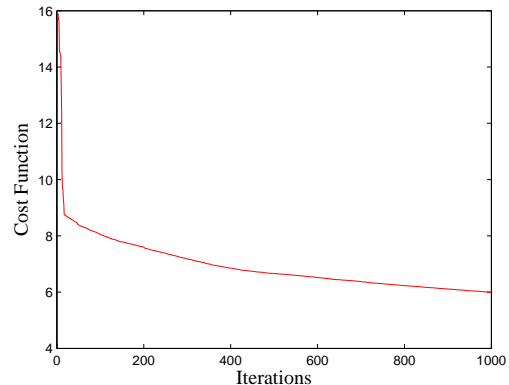
(c) Radiation Pattern for 30 elements



(d) Cost Function for 30 elements



(e) Radiation Pattern for 72 elements



(f) Cost Function for 72 elements

Figure 4.4: Simulation Results of LAA By Relative Distance Optimisation

4.4 Optimisation of PAA by BA

LAA could not work out for the conceived desired split beam. Hence the PAA is used to radiate to give the desired beam. For this purpose array is placed in x-y plane. ϕ is considered as 0° . To get the desired pattern current phase (β) is taken into consideration. Hence appropriate value of β is taken as:

$$\beta = -(-1)^{(N*(m-1)+n)} * \sin(10 * \pi/180)$$

This will give maxima due to alternate elements come on -10° and 10° respectively.

$$AF(\theta) = \sum_{n=1}^N \sum_{m=1}^M \left[I_{mn} * e^{(j(n-1)kdsin\theta cos\phi - (-1)^{(N*(m-1)+n)} * \sin(10*\pi/180))} \right] * \left[e^{(j(m-1)kdsin\theta sin\phi)} \right] \quad (4.2)$$

Fitness function remains the same as discussed in section 4.2.

4.4.1 Amplitude Excitation Optimisation of PAA

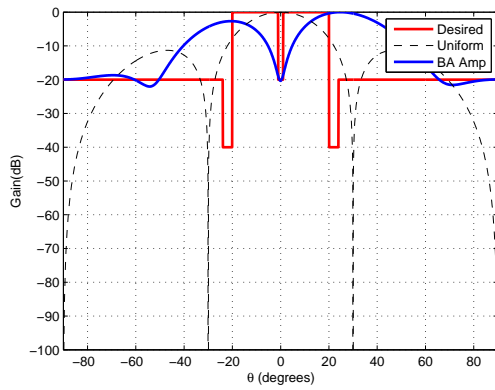
Simulation results of amplitude excitation optimised PAA is shown in Figure 4.5. Radiation pattern is shown in Figure 4.5a, 4.5c and 4.7e and correspondingly their cost function is shown in Figure 4.5b, 4.5d and 4.5f. In the table array size is taken as

Array size = number of elements in a row \times number of elements in a column

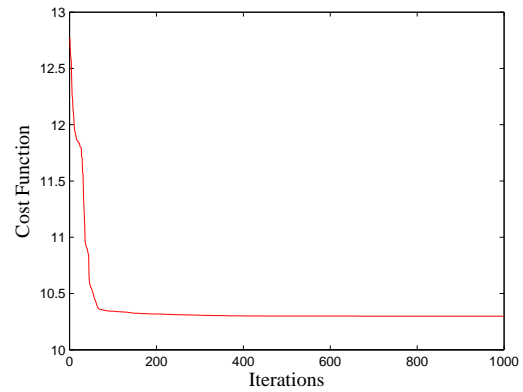
Hence 4x4 means plane contains four elements in a row and four elements in a column and total of 16 elements in a plane. Its SLL and HPBW is shown in Table 4.5. In each case only one main beam is obtained. From the Table 4.5 for 4x4 elements it can be seen that its HPBW is 25.5° which exceeds more than desired. For 8x8 elements HPBW is 11° but its maximum SLL is -3.546 dB which also exceeded from desired. For 10x10 elements HPBW is 10.1° but still maximum SLL is -5.594 dB. From cost function diagrams it is noticed that as number of elements increases convergence rate increases. Hence convergence rate is more in case of 10x10 elements.

No of elements	HPBW(Degree)	SLL(dB)
4x4	25.5	-18.86
8x8	11	-3.546
10x10	10.1	-5.594

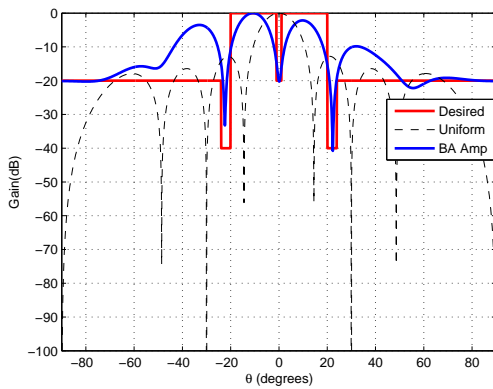
Table 4.5: SLL & HPBW in Amplitude Excitation Optimisation



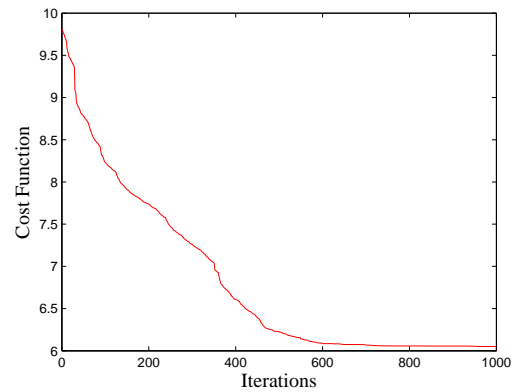
(a) Radiation Pattern for 4x4 elements



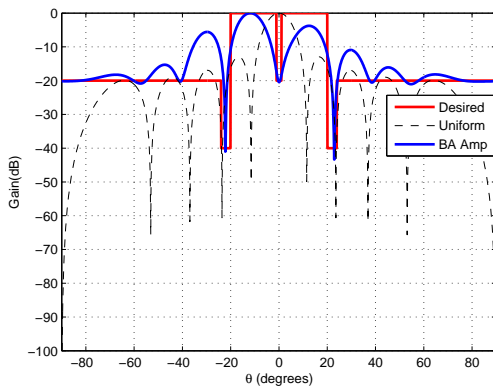
(b) Cost Function for 4x4 elements



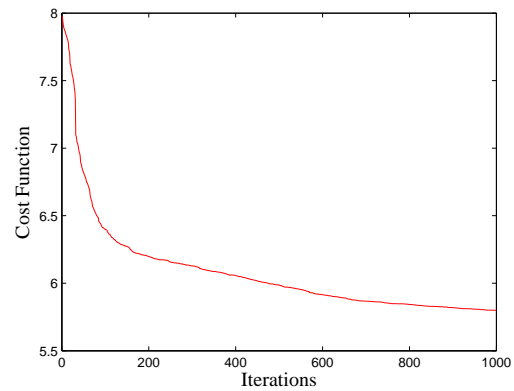
(c) Radiation Pattern for 8x8 elements



(d) Cost Function for 8x8 elements



(e) Radiation Pattern for 10x10 elements



(f) Cost Function for 10x10 elements

Figure 4.5: Simulation Results of PAA By Amplitude Excitation optimisation

No of elements	HPBW(Degree)	SLL(dB)
4x4	25.1	-18.86
8x8	11	-7.33
10x10	10.6	-7.807

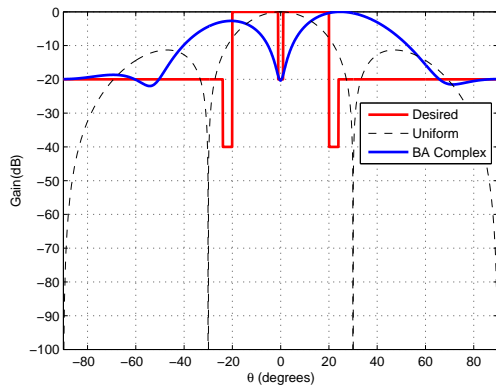
Table 4.6: SLL & HPBW in Complex Excitation Optimisation

4.4.2 Complex Excitation Optimisation of PAA

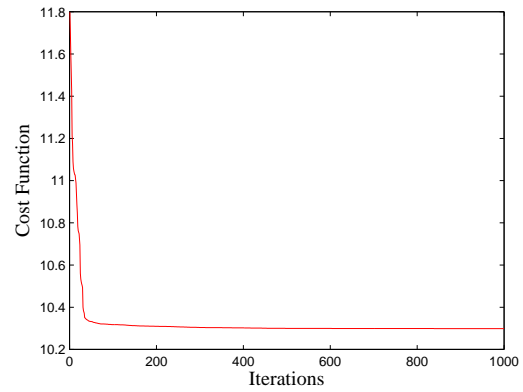
Simulation results for complex amplitude excitation in PAA is shown in Figure 4.6 and its SLL and HPBW is mentioned in Table 4.6 for different number of elements. From the Tables 4.6 and 4.5 it can be seen that HPBW is not improved in complex excitation optimisation and it is almost same as in amplitude excitation optimisation but as number of elements increased maximum SLL is reduced in this case compared to the case of amplitude excitation optimisation discussed in section 4.4.1.

4.4.3 Relative Distance Optimisation in PAA

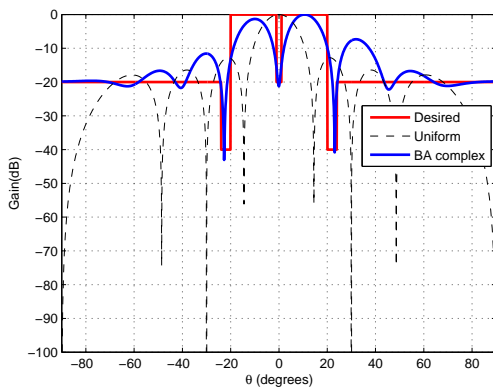
Radiation pattern of relative distance optimised PAA is shown in Figure 4.7 and SLL and HPBW for different number of elements is shown in Table 4.7. From the figure it can be said that relative distance optimisation works better as compared to amplitude excitation optimisation and complex amplitude optimisation. In all the cases two main beams means split beam is obtained. For 4x4 elements two main beams are obtained but two nulls having value -40 dB is not obtained perfectly. In case of 8x8 elements nulls are covered perfectly but max SLL is high and its value is -14.53 dB. For 10x10 elements one null can be obtained perfectly and SLL is reduced to great extent and its value is -17.07 dB. Cost function for relative distance optimisation in PAA is shown in Figures 4.7b, 4.7d and 4.7f. From the figure it can be seen that convergence rate in case of 8x8 elements is more compared to other two cases means for 4x4 elements and for 10x10 elements.



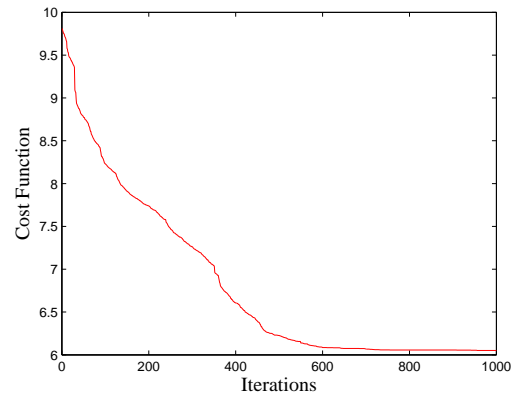
(a) Radiation Pattern for 4x4 elements



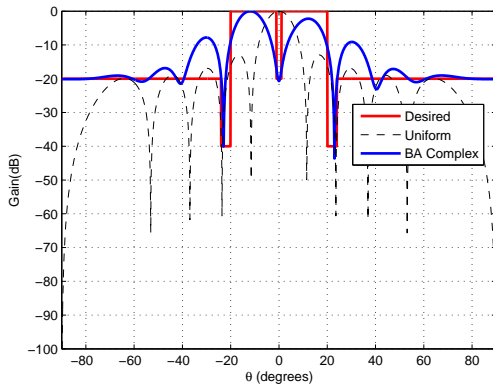
(b) Cost Function for 4x4 elements



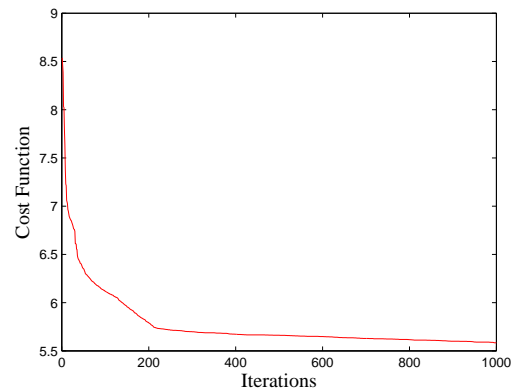
(c) Radiation Pattern for 8x8 elements



(d) Cost Function for 8x8 elements



(e) Radiation Pattern for 10x10 elements

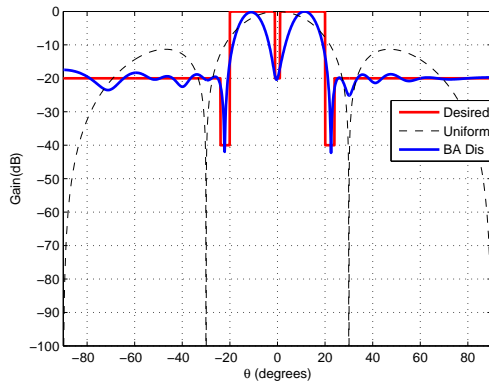


(f) Cost Function for 10x10 elements

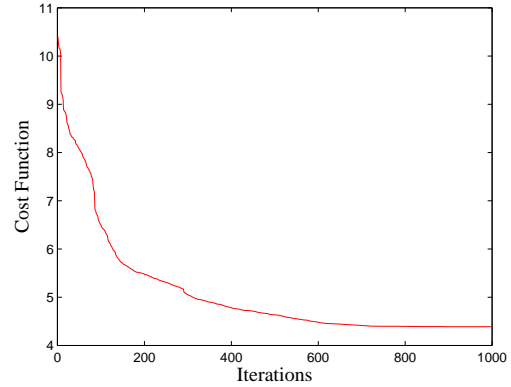
Figure 4.6: Simulation Results of PAA By Complex Excitation optimisation

No of elements	HPBW(Degree)	SLL(dB)
4x4	6.5	-17.8
8x8	7.5	-14.53
10x10	8.3	-17.07

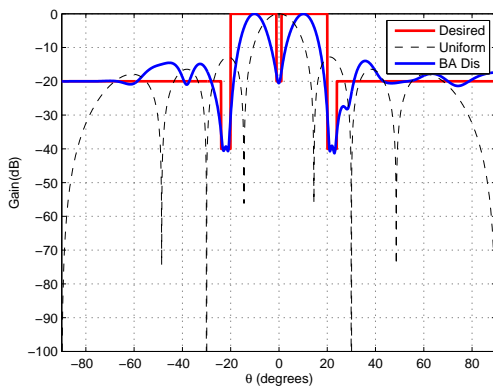
Table 4.7: SLL & HPBW in Relative Distance Optimisation



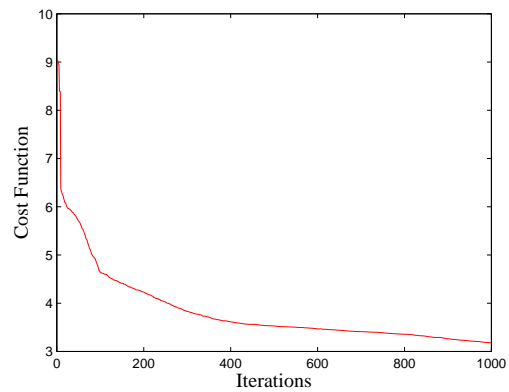
(a) Radiation Pattern for 4x4 elements



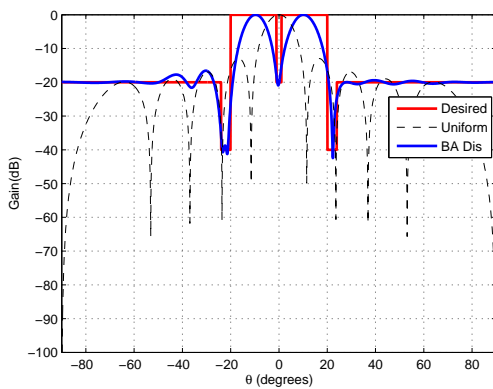
(b) Cost Function for 4x4 elements



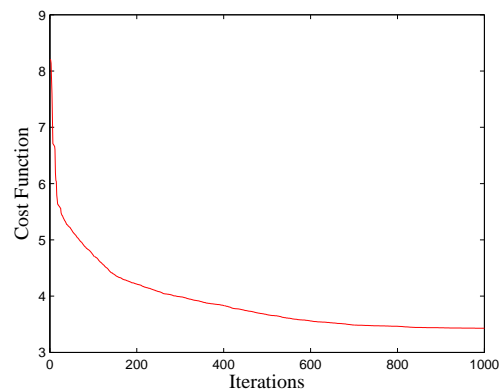
(c) Radiation Pattern for 8x8 elements



(d) Cost Function for 8x8 elements



(e) Radiation Pattern for 10x10 elements



(f) Cost Function for 10x10 elements

Figure 4.7: Simulation Results of PAA By Relative Distance optimisation

No of elements	HPBW(Degree)	SLL(dB)
4x3x6	9	-10
5x3x6	8.7	-14.75
7x3x6	7.8	-17.94

Table 4.8: SLL & HPBW by Amplitude excitation Optimisation

4.5 Optimisation of HPA by BA

Array Factor of HPA is discussed in Section 2.3. It has property of omnidirectional radiation pattern. Hence due to this property it can be used for various purposes. For the desired pattern as discussed in above section it is a very useful type of conformal array. Main advantage of this array does not need steering to get the split beam.

4.5.1 Amplitude Excitation Optimisation of HPA

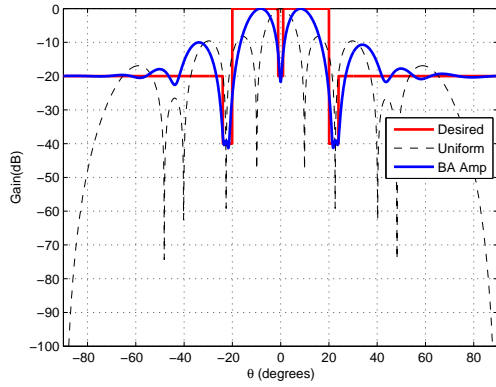
Simulation result of HPA by amplitude excitation optimisation is shown in Figure 4.8. SLL and HPBW is discussed in Table 4.8.

Array size = number of elements in a row \times number of elements in a column \times number of plane(6)

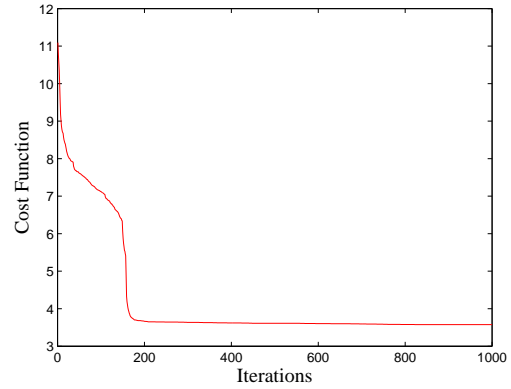
Hence 4x3x6 means each plane contains 4 elements in row and 3 elements in column. From the figures it can be seen that optimised pattern for HPA is better than LAA and PAA. For 4x3x6 elements it can be seen that maximum SLL is more than desired and its value is -10 dB and also nulls between main lobe is not covered properly. For 5x3x6 elements SLL is reduced but more than desired and its value is -14.75. For 7x3x6 elements all nulls are covered properly and SLL is also almost equal to desired value. Its cost function is shown in figure 4.8b, 4.8d and 4.8f. From the diagram it can be seen that convergence rate is more for 7x3x6 elements.

4.5.2 Complex Excitation Optimisation of HPA

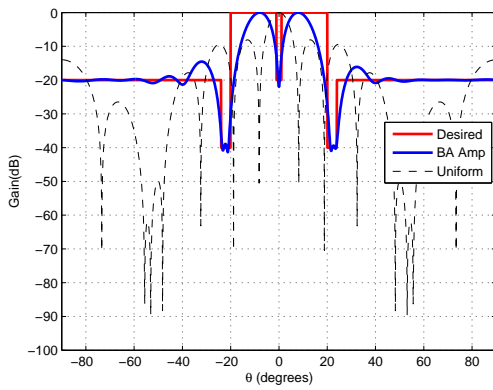
Simulation results for complex excitation optimised HPA is shown in Figure 4.9 and SLL and HPBW is discussed in Table 4.9. From the table it can be seen



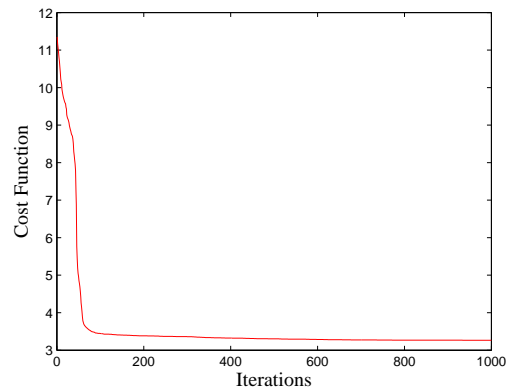
(a) Radiation Pattern for 4x3x6 elements



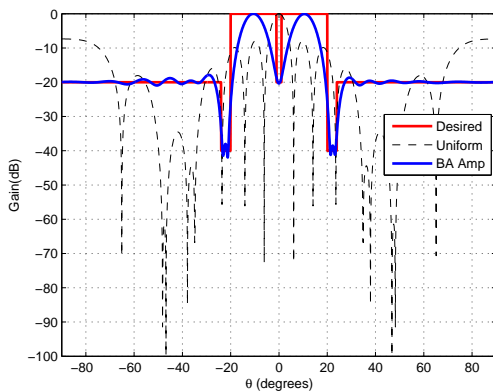
(b) Cost Function for 4x3x6 elements



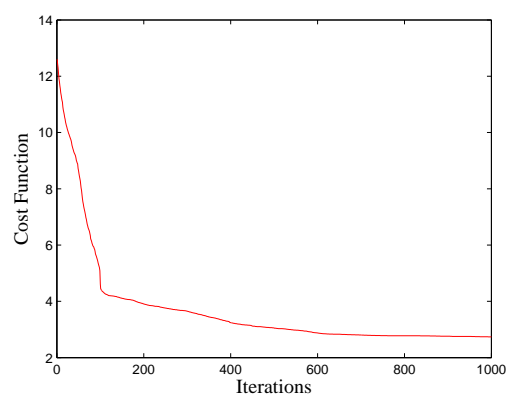
(c) Radiation Pattern for 5x3x6 elements



(d) Cost Function for 5x3x6 elements



(e) Radiation Pattern for 7x3x6 elements



(f) Cost Function for 7x3x6 elements

Figure 4.8: Simulation Results of HPA By Amplitude Excitation optimisation

No of elements	HPBW(Degree)	SLL(dB)
4x3x6	9	-11.48
5x3x6	8.7	-18
7x3x6	7.9	-17.98

Table 4.9: SLL & HPBW by Complex Excitation Optimisation

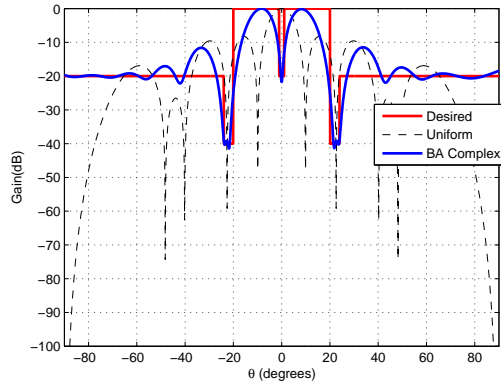
No of elements	HPBW(Degree)	SLL(dB)
4x3x6	8.7	-12.76
5x3x6	8.7	-15.34
7x3x6	7.7	-19.34

Table 4.10: SLL & HPBW by Relative Distance Optimisation

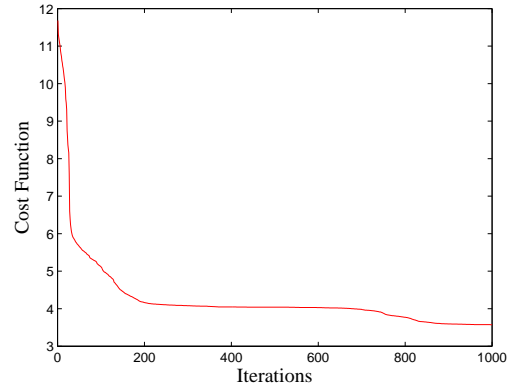
that like LAA and PAA here also HPBW does not vary more compared to amplitude excitation optimisation but SLL reduction is better in this case. For 4x3x6 elements SLL is -11.48 dB which is 3.27 dB less than the amplitude excitation optimisation. For 5x3x6 elements also it is reduced to -18 dB which is -3.25 dB less than the amplitude excitation optimisation. For 7x3x6 SLL is -17.98 dB. If number of elements in a row is 'N' then

length of a plane $= (N + 1) \times \lambda/2$. and antenna elements distance vary from 0 to $N * \lambda/2$. So that last element distance should not be greater than length of a plane. Optimisation is done in both direction it means x and z direction simultaneously.

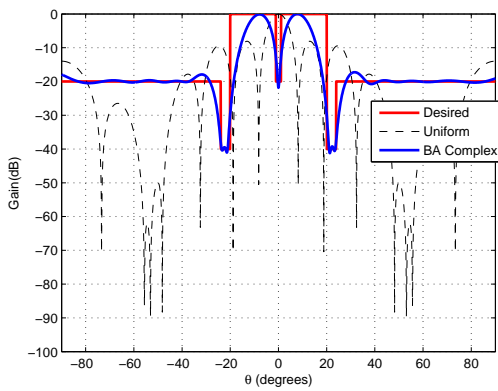
Simulation results for relative distance optimised HPA is shown in Figure 4.10 and SLL and HPBW is discussed in Table 4.10. From the table it can be seen that SLL reduction in relative distance is more in comparison to amplitude excitation and complex excitation optimisation. For 7x3x6 elements SLL is almost equal to desired SLL. It is the advantage of relative distance optimisation.



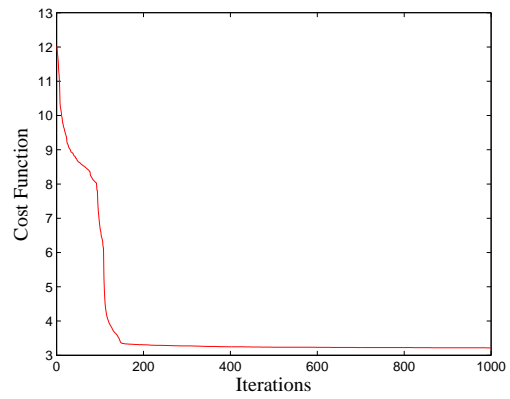
(a) Radiation Pattern for 4x3x6 elements



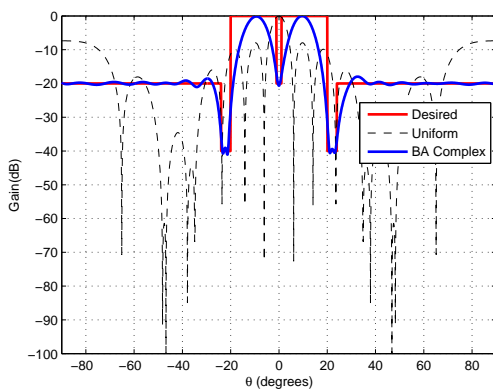
(b) Cost Function for 4x3x6 elements



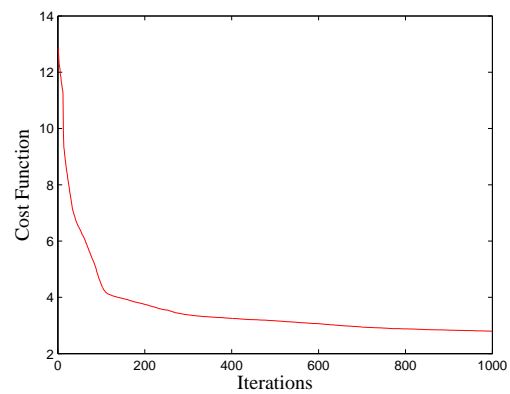
(c) Radiation Pattern for 5x3x6 elements



(d) Cost Function for 5x3x6 elements

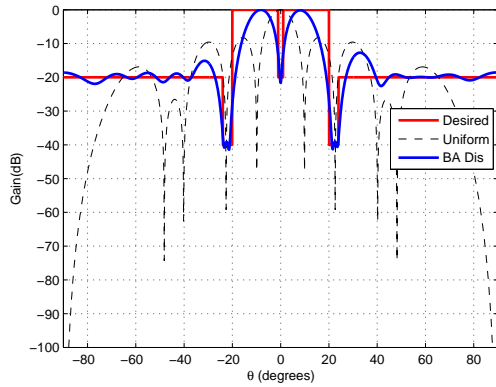


(e) Radiation Pattern for 7x3x6 elements

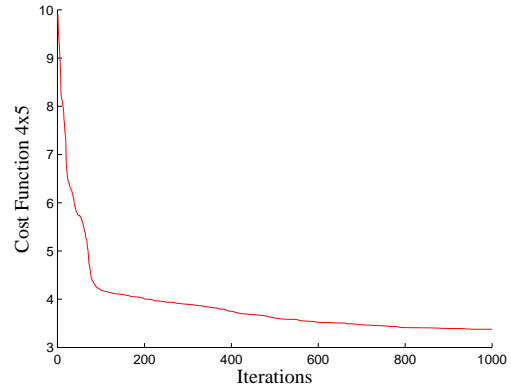


(f) Cost Function for 7x3x6 elements

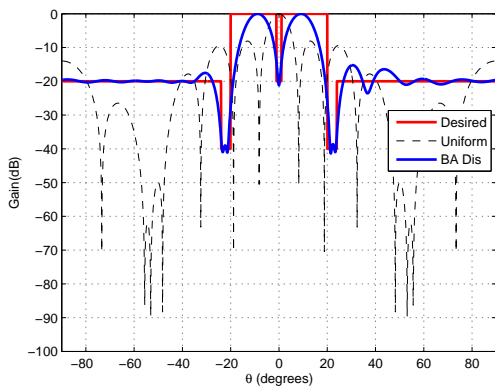
Figure 4.9: Simulation Results of HPA By Complex Amplitude Excitation



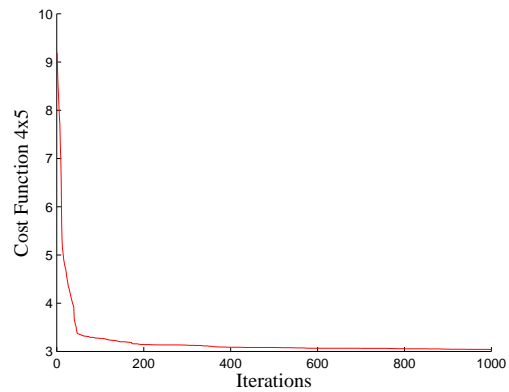
(a) Radiation Pattern for 4x3x6 elements



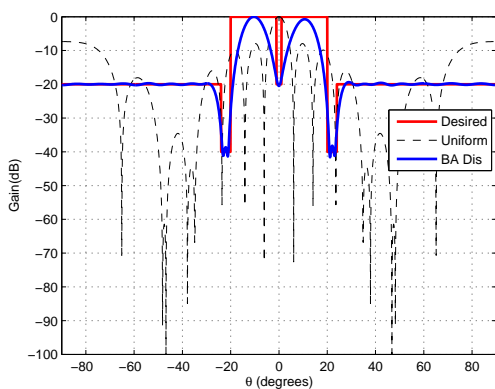
(b) Cost Function for 4x3x6 elements



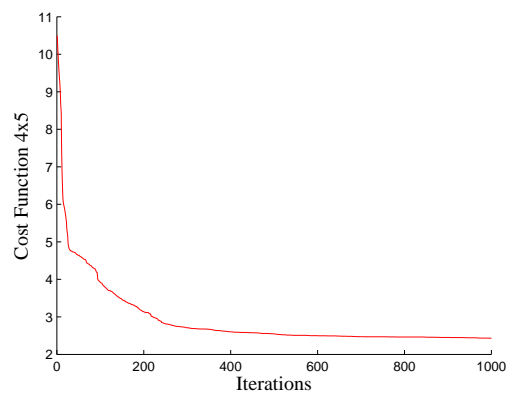
(c) Radiation Pattern for 5x3x6 elements



(d) Cost Function for 5x3x6 elements



(e) Radiation Pattern for 7x3x6 elements



(f) Cost Function for 7x3x6 elements

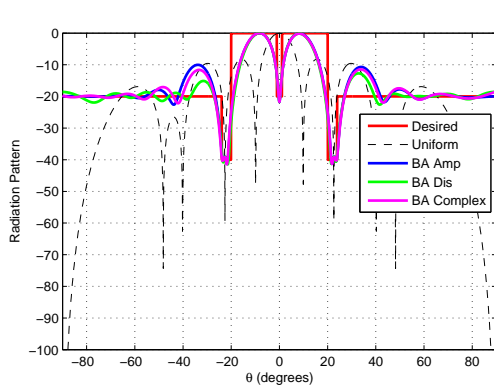
Figure 4.10: Simulation Results of HPA By Relative Distance optimisation

Size	HPBW(degree)			SLL(dB)		
	Amplitude Excitation	Complex Excitation	Relative Distance	Amplitude Excitation	Complex Excitation	relative Distance
4x3x6	9	9	8.7	-10	-11.48	-12.76
5x3x6	8.7	8.7	8.7	-14.75	-18	-15.34
7x3x6	7.8	7.9	7.7	-17.94	-17.98	-19.34

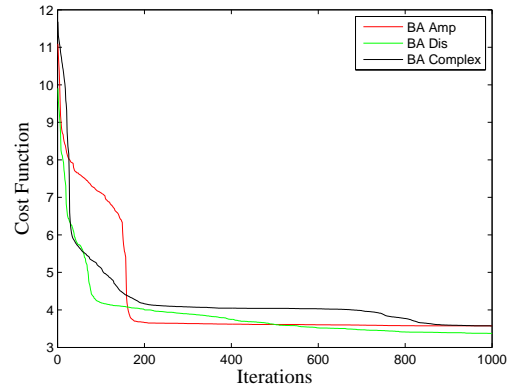
Table 4.11: Comparison of optimisation of different parameters of HPA

4.5.3 Comparative Study of Various controlling parameters of HPA

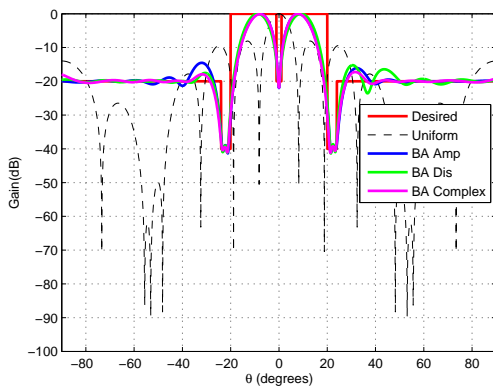
Summarized radiation pattern by amplitude excitation optimisation, complex amplitude excitation and relative distance optimisation is shown in Figure 4.11. Comparative study of optimisation of different controlling parameters of HPA is shown in Table 4.11. In SLL reduction relative distance optimisation leads to complex excitation optimisation followed by than amplitude excitation optimisation. From the cost function diagram also it can be seen that relative distance optimisation. Summarised cost function is shown in Figure 4.11b, 4.11d and 4.11f. From cost function diagram it can be seen that cost convergence rate at a lower value in relative distance optimisation than amplitude excitation optimisation and complex excitation optimisation.



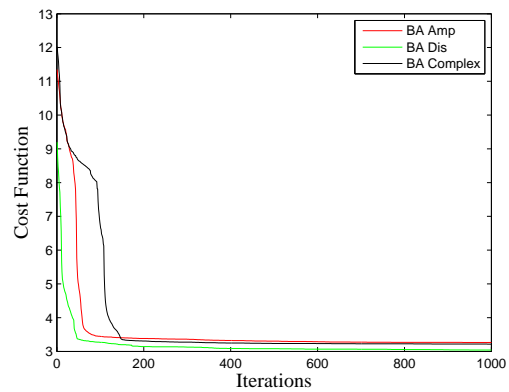
(a) Radiation Pattern for 4x3x6 elements



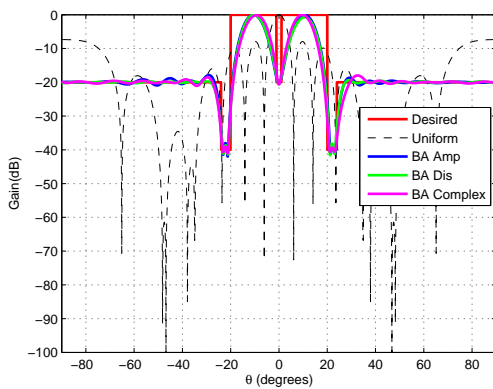
(b) Cost Function for 4x3x6 elements



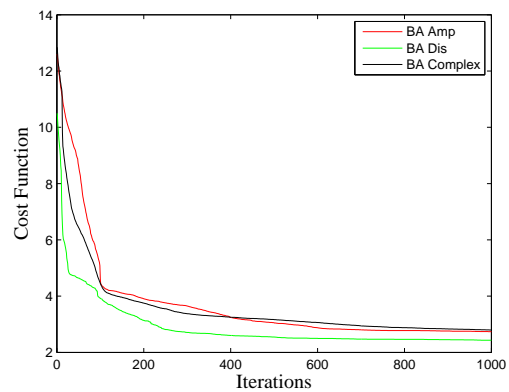
(c) Radiation Pattern for 5x3x6 elements



(d) Cost Function for 5x3x6 elements



(e) Radiation Pattern for 7x3x6 elements



(f) Cost Function for 7x3x6 elements

Figure 4.11: Combined Simulation Results of HPA

4.6 Application

Split beam pattern can be used in Synthetic Aperture Radar(SAR) application [18].Working of split beam in SAR shown in Figure 4.12.SAR uses doppler effect to track the target.In split beam concept it records all data from the echo.As target moves due to change in phase it can detect the target after time T .

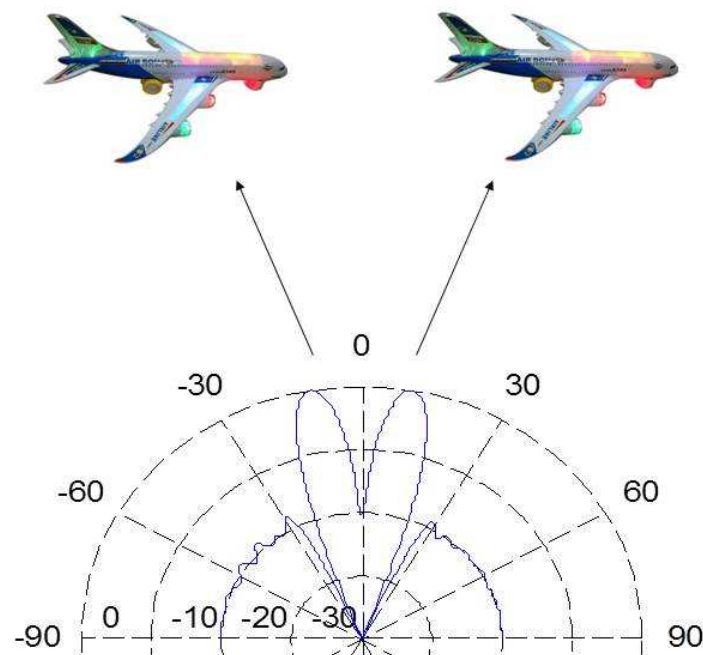


Figure 4.12: Synthetic Aperture Radar

Chapter 5

CST Implementation of HPA

5.1 CST Studio

CST(Computer Simulation Technology) Microwave Studio is the powerful and easy to use electromagnetic field simulation software [20].It offers accurate, efficient computational solutions for electromagnetic design and analysis. This program combines a user friendly interface with unsurpassed simulation performance.

CST Microwave Studio is part of CST Studio Suite.

5.1.1 CST Microwave Studio

CST Microwave studio is a powerful technique is used at low frequency to a high frequency. It uses ASIC modelling which simplifies the process of creating different type of structures in this case HPA and provide graphical modelling like 3-D plot,2-D plot while one of two parameters either θ or ϕ is constant and another will vary.After structure designing automatic meshing procedure is applied before a simulation is started.

CST Microwave studio works on *Method on Demand* which gives the choice of simulate or mesh type which suits for particular problem.

Basic Features of CST Microwave Studio

The following list gives you an overview of main feature of CST Microwave Studio.

1. Native graphical user interface based on Windows XP, Windows Vista , Windows 7 and Linux.
2. Fast and memory efficient Finite Integration Technique.
3. Extremely good performance due to Perfect Boundary Approximation (PBA). Feature to solve for solver using hexahedral grid. The transient and eigenmode solver also support the Thin Sheet Technique (TST).
4. The structure can be viewed either as a 3D model or as a schematic. The latter allows for easy coupling of EM simulation with circuit simulation.

5.1.2 Patch dipole

Patch antennas are low cost, have a low profile and are easily fabricated antenna. Due to simple structure it is widely used in telecommunication. It is widely used in cellular mobile communication. Also it is useful in designing of different types of array like linear array, circular array and planar array. These days it is widely used in conformal array designing.

In this paper HPA is designed using patch antenna. Frequency is fixed as 2.4 GHz. Substrate is taken as Teflon and patch is made up of copper (annealed). Patch dipole parameters are shown in table 5.1. It is created in CST and after that used in HPA. The directivity of patch dipole is 3.9 dBi and main lobe direction is 90° . These are very useful results in construction of other structure using patch.

Parameters of patch is discussed below [21].

$$\text{width of patch} = 2 * w_1 + s_2 = 2 * 20.8 + 3 = 44.6 \text{mm} \quad (5.1)$$

$$\text{height of patch} = h_1 + h_2 + h_3 + h_4 = 6 + 3 + 16 + 12 = 37 \text{mm} \quad (5.2)$$

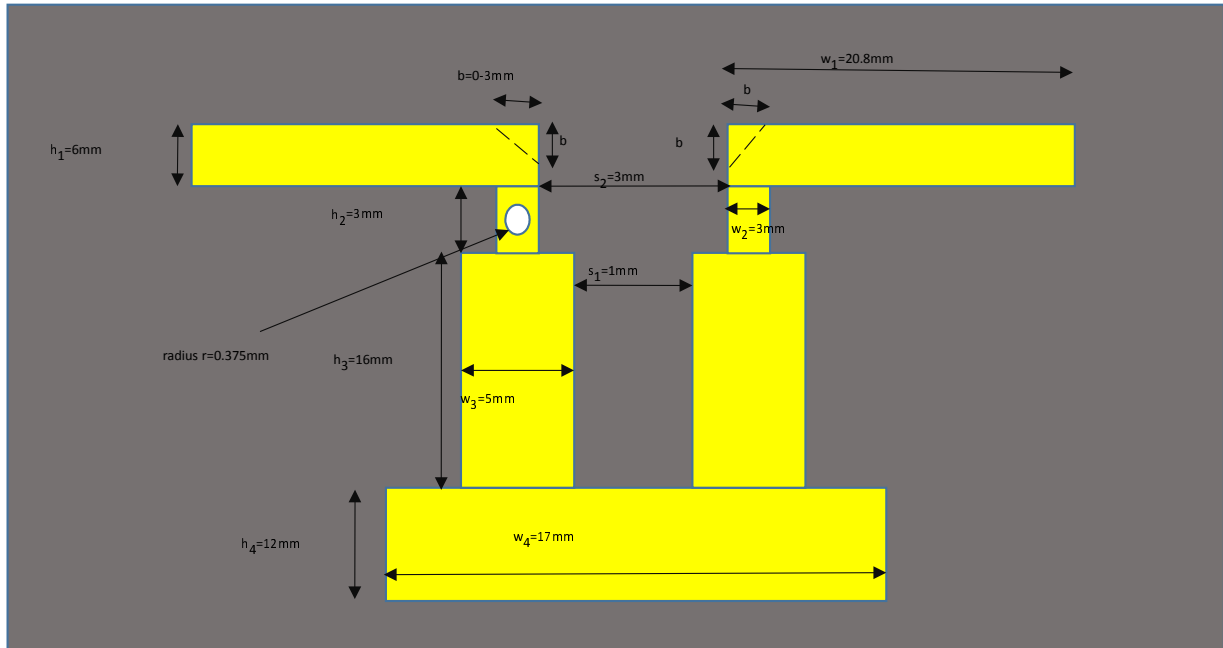


Figure 5.1: Patch Antenna

Parameter	Value in mm
length of strips	$h_1 = 6$ $h_2 = 3$ $h_3 = 32$ $h_4 = 16$
width of strips	$w_1 = 20.8$ $w_2 = 3$ $w_3 = 5$ $w_4 = 17$
radius of circle	$r = 0.375$
micro-strip bend	$b (0-3)$
Spacing between arms	$s_1=1$ $s_2=3$

Table 5.1: Parameters Used in Designing the Patch

Electric field equation for patch dipole is given as

$$E_{\theta} = \frac{\sin(kw \sin \theta \sin \phi / 2)}{kw \sin \theta \sin \phi / 2} * \cos(kL \sin \theta \cos \phi / 2) * \cos \phi \quad (5.3)$$

$$E_{\phi} = \frac{\sin(kw \sin \theta \sin \phi / 2)}{kw \sin \theta \sin \phi / 2} * \cos(kL \sin \theta \cos \phi / 2) * \cos \theta \sin \phi \quad (5.4)$$

5.1.3 Implementation HPA in CST

For designing of HPA in CST its dimension should be known. Dimension of HPA depends number of patch antenna used for designing and distance between the adjacent patches.

HPA synthesis is done for 24 antenna elements. The antenna elements are placed in such manner that each plane consist 4 element. Each antenna placed at $\lambda/2$ distance with its adjacent antenna elements. Hexagonal shape containing six side so number of elements would we 24. Height and width of plane is calculated using parameters from equation 5.1 and 5.2.

$$\begin{aligned}\lambda &= \frac{c}{f} \\ \lambda &= \frac{3*10^8}{2.4*10^9} \\ &= 0.125 \text{ m} = 125 \text{ mm}\end{aligned}$$

*width of one plane = 2*width of patch(in mm)+2*Distance between two element(in mm)*

$$\begin{aligned}&= 2*44.6 + 2* \lambda/2 \\ &= 214.2 \text{ mm}\end{aligned}$$

height of one plane = 2 height of patch (in mm)+2*Distance between two element (in mm)*

$$\begin{aligned}&= 2*37 + 2* \lambda/2 \\ &= 199 \text{ mm}\end{aligned}$$

Then initially a plane is creating having height and width discussed above of Teflon from CST library. Then inserting patch at $\lambda/2$ distance to each other and $\lambda/4$ distance from the end of the plane. Taking six similar plane and use translational property to create HPA using patch. After port is created in each patch and the design is completed then simulation is done. Then combined result is obtained by post processing.

Geometric view of HPA using CST for 2x2x6 means 24 elements is shown in Figure 5.2.3-D radiation pattern is shown in Figure 5.3. Its overall directivity directivity is 6.878 dBi.

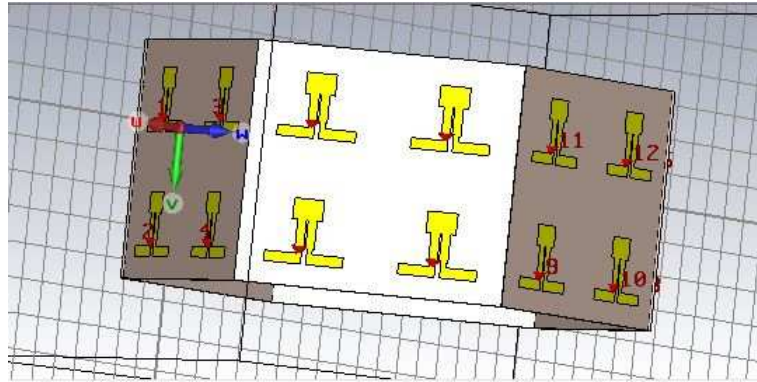


Figure 5.2: Geometric View of HPA Using CST Studio

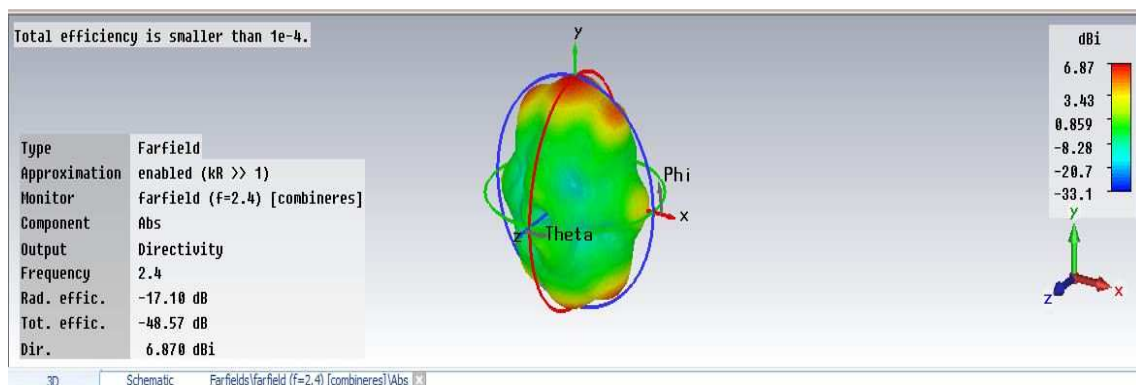


Figure 5.3: 3-D Radiation Pattern of HPA in CST

5.1.4 Comparision Between CST and MATLAB

HPA is constructing in CST and also its radiation pattern is obtained by using the simulation using MATLAB. Both results are compared in this section. Figure 5.4 shows the radiation pattern using CST and Figure 5.5 shows radiation pattern using MATLAB at $\phi=0$. Although both pattern is not matching perfectly due to consideration of lossy substrate in CST but lossless in MATLAB. But these have some similiarity.

1. Both pattern have five lobes.
2. Main lobe in both cases placed between 80 to 100.

Another pattern is shown in Figure 5.6 using CST and 5.7 using MATLAB for $\phi=90$. These have also some similiarity.

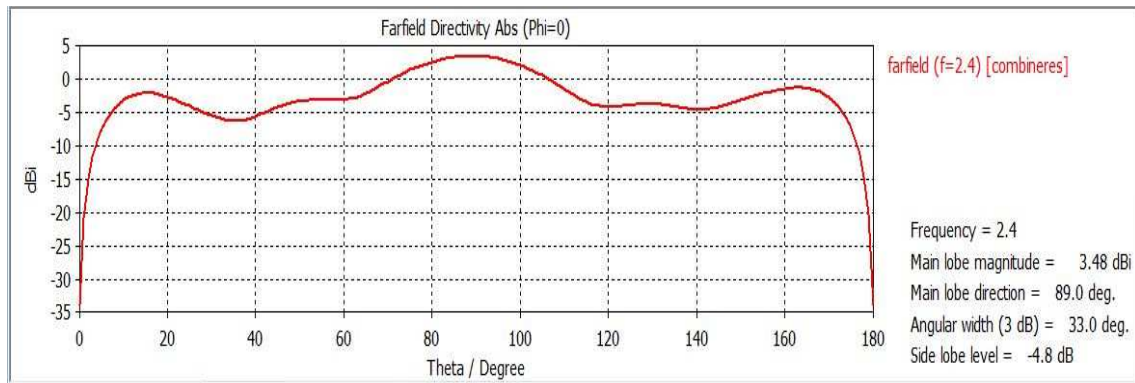


Figure 5.4: Radiation Pattern at phi=0 in CST

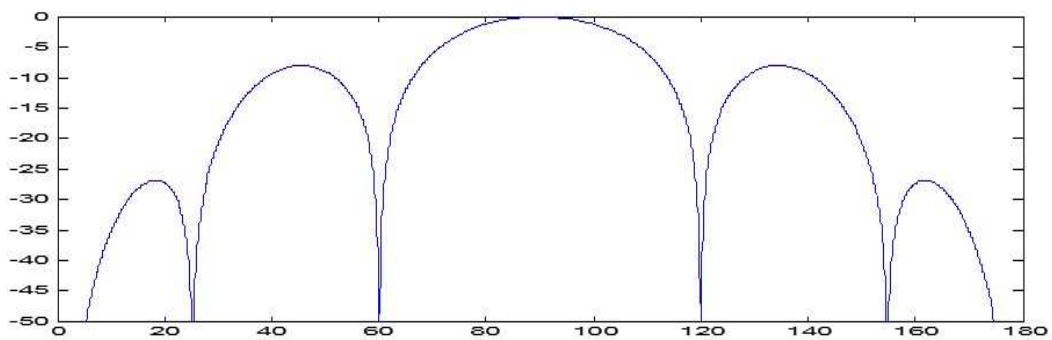


Figure 5.5: Radiation Pattern at phi=0 in MATLAB

1. Both have three lobes.
 2. Main lobe placed between approx between 40 to 140.
- other radiation patterns are shown in Figure 5.8 and 5.9.

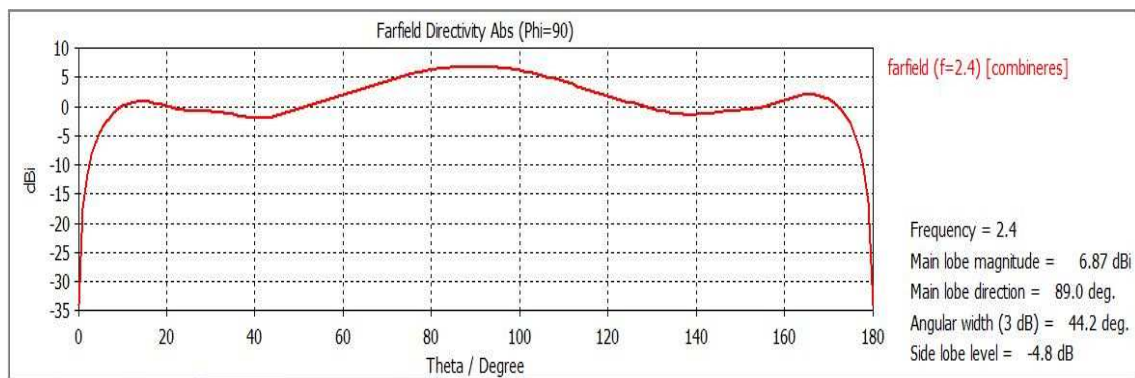
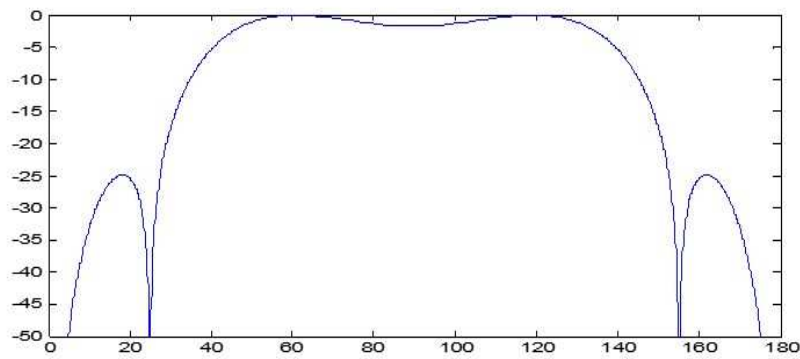
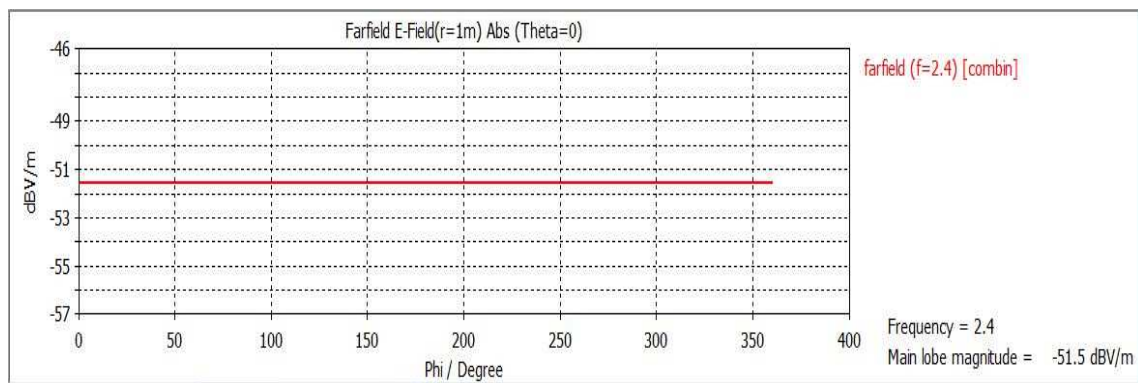
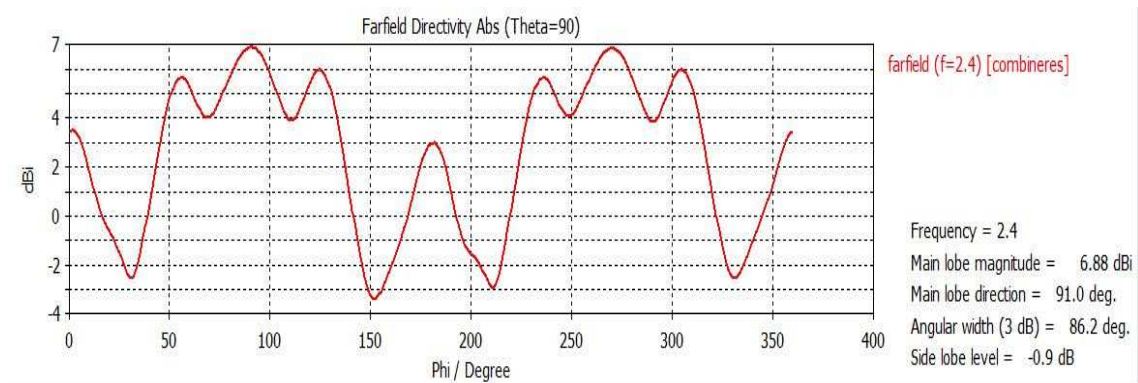


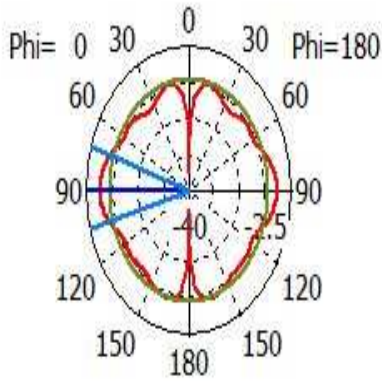
Figure 5.6: Radiation Pattern at phi=90 in CST

Figure 5.7: Radiation Pattern at $\phi=90$ in MATLABFigure 5.8: Radiation Pattern at $\theta=0$ in CSTFigure 5.9: Radiation Pattern at $\theta=90$ in CST

Polar plot of HPA using CST is shown in Figure 5.10a, 5.10b, 5.10c and 5.10d. From the polar plots it can be noticed that main lobe obtained at 90° with respect to elevation angle (θ) at constant azimuthal angle (ϕ). While provide omnidirectional pattern with respect to azimuthal angle (ϕ) if elevation

angle(θ) is 0^0 . If $\phi = 0$ then maxima is obtained at 90^0 and 270^0 .

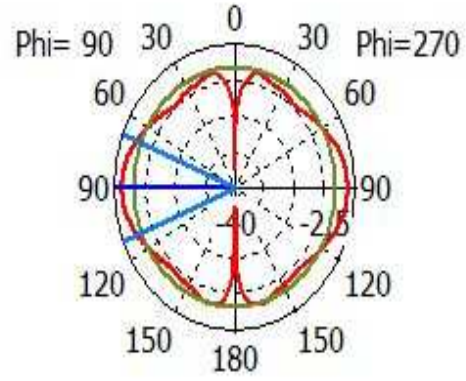
Farfield Directivity Abs (Phi=0)



Theta / Degree vs. dBi

(a) Polar Plot at Phi=0

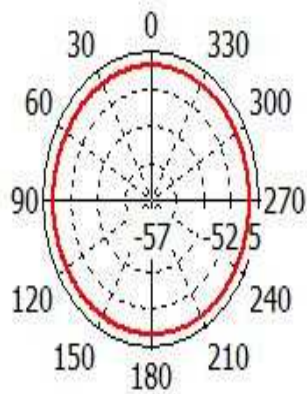
Farfield Directivity Abs (Phi=90)



Theta / Degree vs. dBi

(b) Polar Plot at Phi=90

Farfield E-Field(r=1m) Abs (Theta=0)



Phi / Degree vs. dBV/m

(c) Polar Plot at theta=0

Farfield Directivity Abs (Theta=90)



Phi / Degree vs. dBi

(d) Polar Plot at Phi=90

Figure 5.10: Polar Plot of HPA using CST

Return loss diagram of HPA is shown in Figure 5.11. From this diagram it can be seen that frequency range is used from 0 to 4 GHz and HPA works on resonant frequency of 2.4 GHz. As it proceeds towards resonant frequency return loss is minimised and it is less than -10 dB.

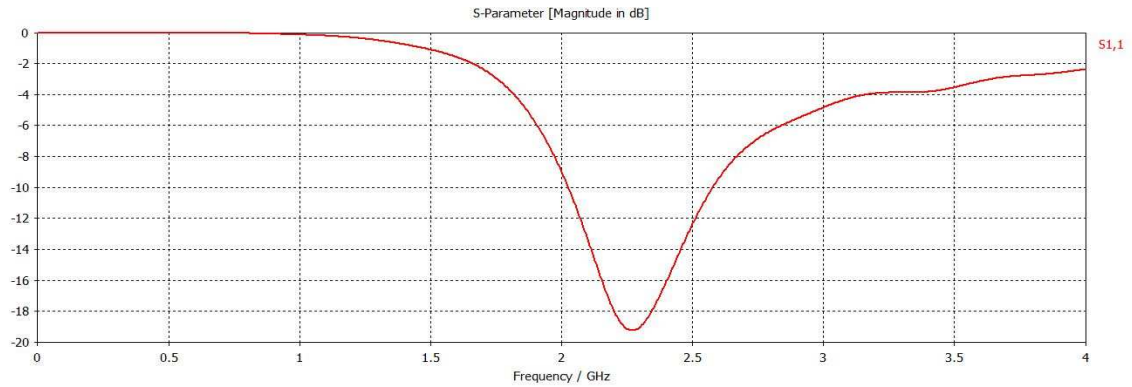


Figure 5.11: Return Loss in HPA

Chapter 6

HPA Synthesis Using Graphical User Interface(GUI)

Graphical user interface allows user to give input and get the output. There is no need to know about programme for user which is embedded. In this section also different input parameter like 'M', 'N' of HPA and 'Iteration', 'Best Run', 'Loudness' and 'Pulse rate' of BA is inserted and get different output parameter like 'HPBW', 'SLL', 'Cost Function' and 'Radiation Pattern'. In Figure 6.1 GUI for HPA using BA is shown.

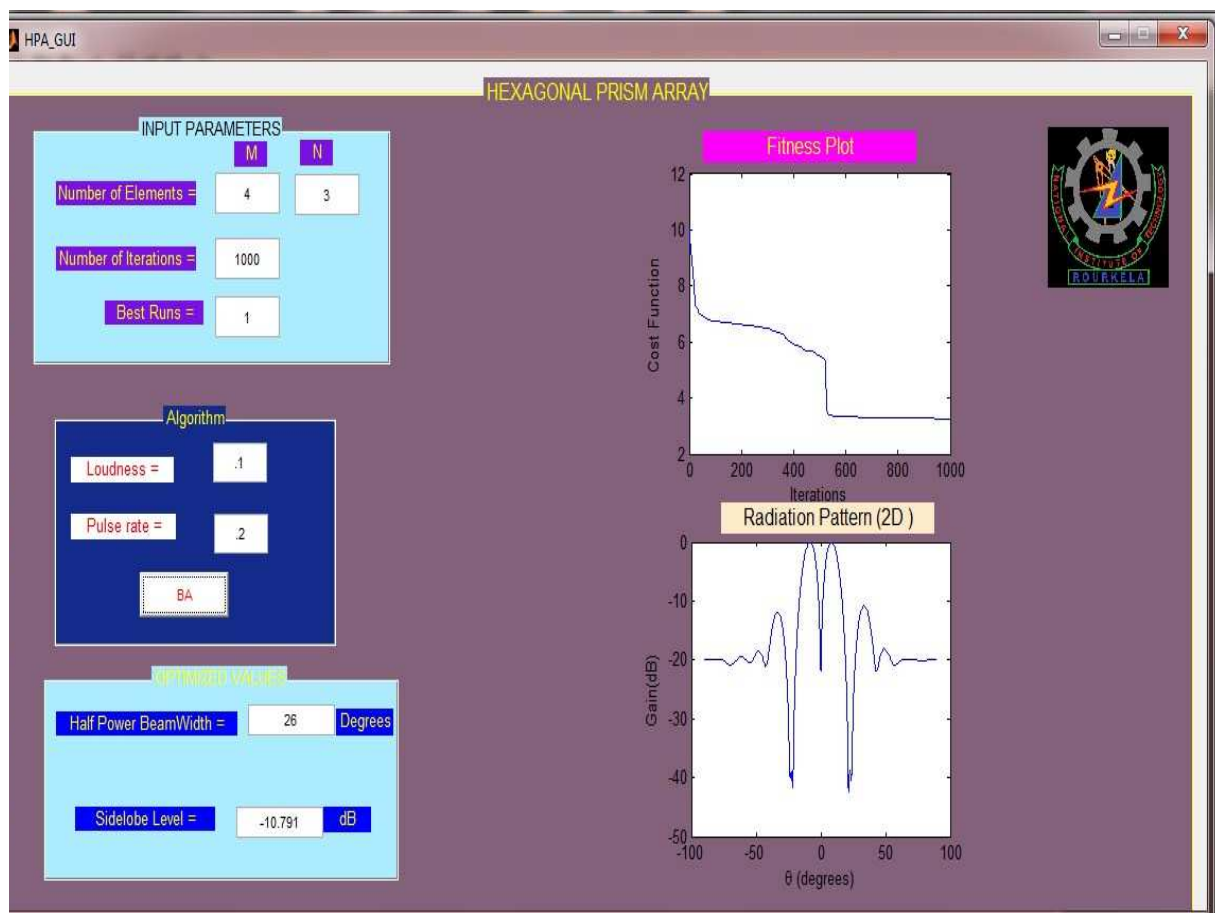


Figure 6.1: Simulation Results of HPA in GUI

Chapter 7

Conclusion And Future Scope

7.1 Conclusion

In this thesis different antenna array like LAA,PAA and HPA controlling parameters are optimised using HPA.For HPA array factor formulation is done using shifting and rotational properties of arrays.Split beam is generated by optimising controlling parameters means excitation and relative distance of LAA,PAA and HPA using BA.In all the cases means in LAA,PAA and HPA relative distance optimisation leads to complex excitation optimisation followed by amplitude excitation optimisation.It is difficult to get split beam in LAA and PAA without steering while in HPA split beam is generated without steering.In LAA and PAA only relative distance optimisation provide split beam, amplitude excitation optimisation and complex excitation optimisation is unable to provide split beam properly.Split beam used in HPA can be used in synthetic aperture radar(SAR).In SAR by using phase change it is able to find the target.

7.2 Limitations

In this thesis mutual coupling is neglected and calculation is done only for far field which has a great impact on radiation pattern and it may be dif-

fer from the desired pattern. For simulation purpose isotropic elements are considered. Structure complexity of considered geometry (HPA) is more when compared to the conventional ones (LAA and PAA).

7.3 Future Scope

In this thesis isotropic elements are considered for simulation. For the practical point of view radiating elements like patch dipole can be considered and implemented. HPA is combination of six planar arrays. Hence it can be used to give omnidirectional pattern or some specific desired pattern using BA or any other algorithm which can be used in satellite and radar communication. Split beam pattern calculation can be done with mutual coupling and for near field.

BA can be modified to give desired pattern for less number of elements. Another algorithm (like PSO or GA) or geometry (like cylindrical array, spherical array) can be introduced to get split beam pattern.

Split beam generated using HPA can be used in satellite and Radar communication.

Bibliography

- [1] John D Kraus. *Antennas*. 1988.
- [2] Sophocles J Orfanidis. *Electromagnetic waves and antennas*. Rutgers University, 2002.
- [3] Constantine A Balanis. *Antenna theory: analysis and design*. John Wiley & Sons, 2012.
- [4] CL Dolph. A current distribution for broadside arrays which optimizes the relationship between beam width and side-lobe level. *Proceedings of the IRE*, 34(6):335–348, 1946.
- [5] AI Uzkov. An approach to the problem of optimum directive antenna design. In *Comptes Rendus (Doklady) de l'Academie des Sciences de l'URSS*, volume 53, pages 35–38, 1946.
- [6] Lars Josefsson and Patrik Persson. *Conformal array antenna theory and design*, volume 29. John wiley & sons, 2006.
- [7] Majid M Khodier and Christos G Christodoulou. Linear array geometry synthesis with minimum sidelobe level and null control using particle swarm optimization. *Antennas and Propagation, IEEE Transactions on*, 53(8):2674–2679, 2005.
- [8] Majid M Khodier and Mohammad Al-Aqeel. Linear and circular array optimization: A study using particle swarm intelligence. *Progress In Electromagnetics Research B*, 15:347–373, 2009.
- [9] Ali Reza Mehrabian and Caro Lucas. A novel numerical optimization algorithm inspired from weed colonization. *Ecological Informatics*, 1(4):355–366, 2006.
- [10] Lotfi Merad, Fethi Bendimerad, and Sidi Meriah. Design of linear antenna arrays for side lobe reduction using the tabu search method. *The International Arab Journal of Information Technology*, 5(3):219–222, 2008.
- [11] Keen-Keong Yan and Yilong Lu. Sidelobe reduction in array-pattern synthesis using genetic algorithm. *Antennas and Propagation, IEEE Transactions on*, 45(7):1117–1122, 1997.
- [12] Iztok Fister Jr, Xin-She Yang, Iztok Fister, Janez Brest, and Dušan Fister. A brief review of nature-inspired algorithms for optimization. *arXiv preprint arXiv:1307.4186*, 2013.
- [13] Xin-She Yang. A new metaheuristic bat-inspired algorithm. In *Nature inspired cooperative strategies for optimization (NICSO 2010)*, pages 65–74. Springer, 2010.
- [14] Aliasghar Baziar, Abdollah Kavooosi-Fard, and Jafar Zare. A novel self adaptive modification approach based on bat algorithm for optimal management of renewable mg. *Journal of Intelligent Learning Systems and Applications*, 5:11–18, 2013.

- [15] Xin-She Yang and Amir Hossein Gandomi. Bat algorithm: a novel approach for global engineering optimization. *Engineering Computations*, 29(5):464–483, 2012.
- [16] Huan Chen. A novel bat algorithm based on differential operator and lévy flights trajectory. *Computational intelligence and neuroscience*, 2013, 2013.
- [17] Teodoro C Bora, Leandro dos S Coelho, and Luiz Lebensztajn. Bat-inspired optimization approach for the brushless dc wheel motor problem. *Magnetics, IEEE Transactions on*, 48(2):947–950, 2012.
- [18] Nicolas Gebert, Gerhard Krieger, and Alberto Moreira. Digital beamforming on receive: techniques and optimization strategies for high-resolution wide-swath sar imaging. *Aerospace and Electronic Systems, IEEE Transactions on*, 45(2):564–592, 2009.
- [19] Radio Engineers Transaction. Frequency independent split beam antenna, March 28 1961. US Patent 2,977,597.
- [20] CST Microwave Studio. Computer simulation technology. *Darmstadt, Germany*, 2009.
- [21] Constantinos Votis, Vasilis Christofilakis, and Panos Kostarakis. Geometry aspects and experimental results of a printed dipole antenna. *International Journal of Communications, Network & System Sciences*, 3(2), 2010.

ABOUT THE AUTHOR

Pawan Kumar was born to Mr. Rajkumar Prasad and Mrs. Urmila Devi on 8th January 1989 in Nalanda District of Bihar. He completed his Bachelor Degree in Electronics and Communication from RKDF IST BHOPAL in 2011. He joined the Department of Electrical Engineering in National Institute of Technology, Rourkela in July 2011 to pursue M.Tech.